THE AERONUTRONIC SELF-OPTIMIZING AUTOMATIC CONTROL SYSTEM

G. Wm. Anderson, R. N. Buland,
and G. R. Cooper

Aeronutronic Systems, Inc.
Glendale, California

SECTION 1

INTRODUCTION

Aeronutronic System's participation in the adaptive autopilot program began with a contract award in February 1957. This contract called for a feasibility study and analysis of the stability augmentation system to be outlined in this report. Successful demonstration of this approach led to a contract extension for further study and for the fabrication and flight test of a portion of the self-adaptive system. This equipment to be flight tested is designed to continuously measure a system's dynamic performance under normal operating conditions. An experimental model has been fabricated and is presently undergoing shakedown tests. Flight tests in an F-100 aircraft will begin in May of this year.

1.1 BASIC CONCEPTS

The concept of the self-adaptive control system is based on the premise that either implicitly or explicitly such a system must perform the operations shown in Figure 1-1:

1) Continuous measurement of system dynamic performance.

2) Continuous evaluation of performance on the basis of some predetermined criterion.

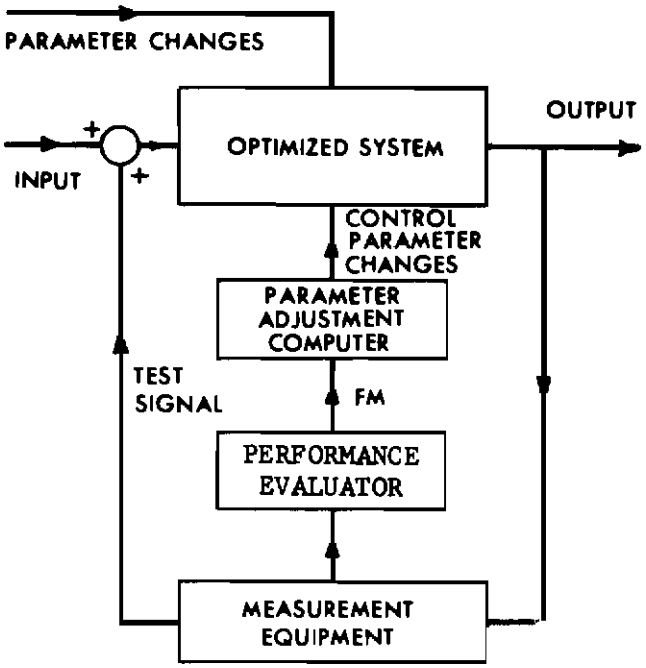

FIGURE 1-1. BASIC SELF-OPTIMIZING SYSTEM

3) Continuous readjustment of system parameters for optimum system performance in accordance with the measurement and the evaluation performed.

Our self-adaptive system consists of an explicit mechanization of these functions.

The measurement of performance should be accomplished with minimum disturbance to the system being optimized. Furthermore, the measurement itself should be relatively immune to the effects of corrupting noise signals. These considerations, in general, lead to the rejection of such standard techniques as are used in the laboratory, including the direct measurement of step or impulse response or the determination of response to steady sinusoidal excitation.

Evaluation of the system's performance can be accomplished by generating a figure of merit from the performance measurement. A figure of merit is defined here as some mathematical function of the measured response, the function being chosen to give emphasis to the specifications of dominant interest.

The most desirable type of FM is one which has zero value when the basic system is "optimally" adjusted and assumes positive or negative values depending on the direction of deviation as the adjustment deviates from "optimum". Such a FM can serve as the adaptive loop's error signal in the true feedback sense and is to be preferred over a FM which has a maximum or minimum at the "optimum" condition. The selection of the proper figure of merit depends mainly on the definition of optimum system performance.

The third operation required of the adaptive loop will vary somewhat with the system being "optimized". Some function (or functions) of the FM must be used to adjust one or more parameters of the "optimized" system.

1.2 PERFORMANCE MEASUREMENT

Several measurement schemes were considered, but the method finally selected depends on a correlation technique usually attributed to Y. W. Lee. If a physical system having an impulse response, $g(t)$, is excited by a noise signal having an autocorrelation function, $\varphi_{ii}(\tau)$, then

$$\varphi_{io}(\tau) = \int_{-\infty}^{\infty} g(t)\, \varphi_{ii}(\tau - t)\, dt \qquad (1.1)$$

where $\varphi_{io}(\tau)$ is the crosscorrelation function of the system input and output. If the excitation noise has a bandwidth considerably larger (three to ten times) than that of the system under test, then $\varphi_{ii}(\tau)$ is effectively an impulse and

$$\varphi_{io}(\tau) = g(\tau) \qquad (1.2)$$

Hence each channel of crosscorrelation provides one point on the impulse response of the system in question.

This approach appears to be ideal for our purposes. The correlation function should be immune to both command signals and to the corruptive signals since the outputs will be uncorrelated with the random noise input. Furthermore, the use of noise excitation allows the excitation energy to be spread over a band of frequencies, and it is expected that the noise amplitude can be kept low enough so that it will only cause a minimum disturbance to the system and pilot.

1.3 PERFORMANCE EVALUATION

The idea of a figure of merit is a fairly common one to the control systems engineer. The most common example is probably the mean square error criterion applied to systems with statistical inputs. A figure of merit which we have considered in some detail employs the damping ratio or relative stability as the criterion for systems performance. As shown in Figure 1-2, it is based on the ratio of the areas of the positive and negative portions of the impulse response and results in a positive or negative quantity as the system damping becomes greater or less than some desired value. By varying the constant K the figure of merit can be made null for different damping ratios. Since the figure of merit reduces to a null for the desired damping ratio and is essentially phase sensitive on either side of the null, this quantity is a suitable error signal for the optimizing system.

AREA RATIO FIGURE OF MERIT

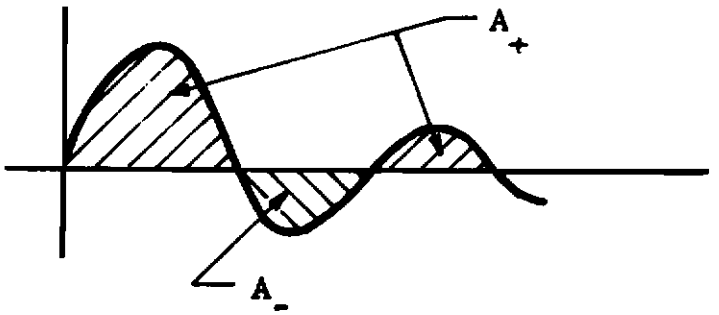

$$F.M. = A_+ + kA_-$$

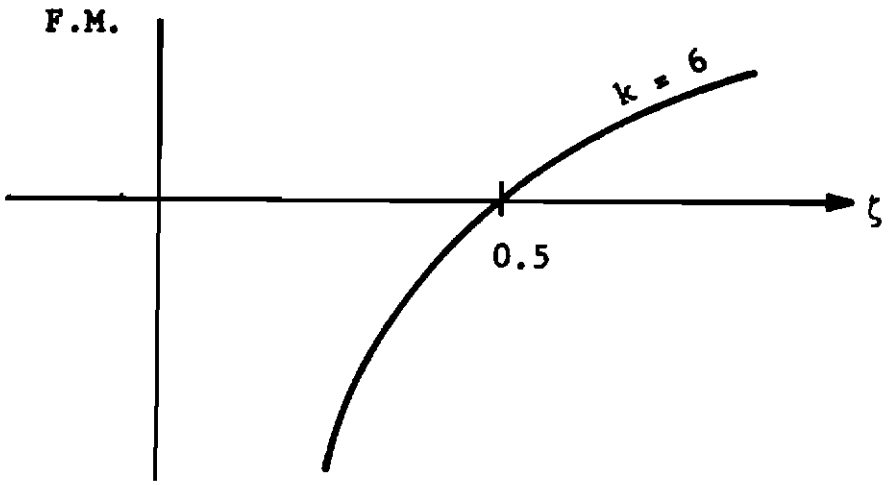

FIGURE 1-2. AREA RATIO FIGURE OF MERIT

1.4 PARAMETER ADJUSTMENT

Controller design may vary somewhat from system to system. In an attempt to develop a universal controller, we investigated the pitch mode of two century series aircraft. A control system which seemed suitable for both aircraft is shown in the block diagram of Figure 1-3. In addition to its being more amenable to a single control parameter, the system was chosen because it behaved more nearly like a second order system. The pole-zero configuration is shown for a typical flight condition. Damping of the dominant pole pair is maintained constant by varying the gain parameter K_a and the compensation time constan T_a.

1.5 SUMMARY

The major emphasis in our program has been placed on the development of the system response measuring equipment. As noted, approaches to the problems of performance evaluation and compensation control have been investigated and found to be feasible, however, considerable work remains to be done in these areas. In the balance of this report, we will present a rather detailed discussion of the theory underlying the approach set forth here, followed by a discussion of the hardware developed and the simulation studies conducted to support this program.

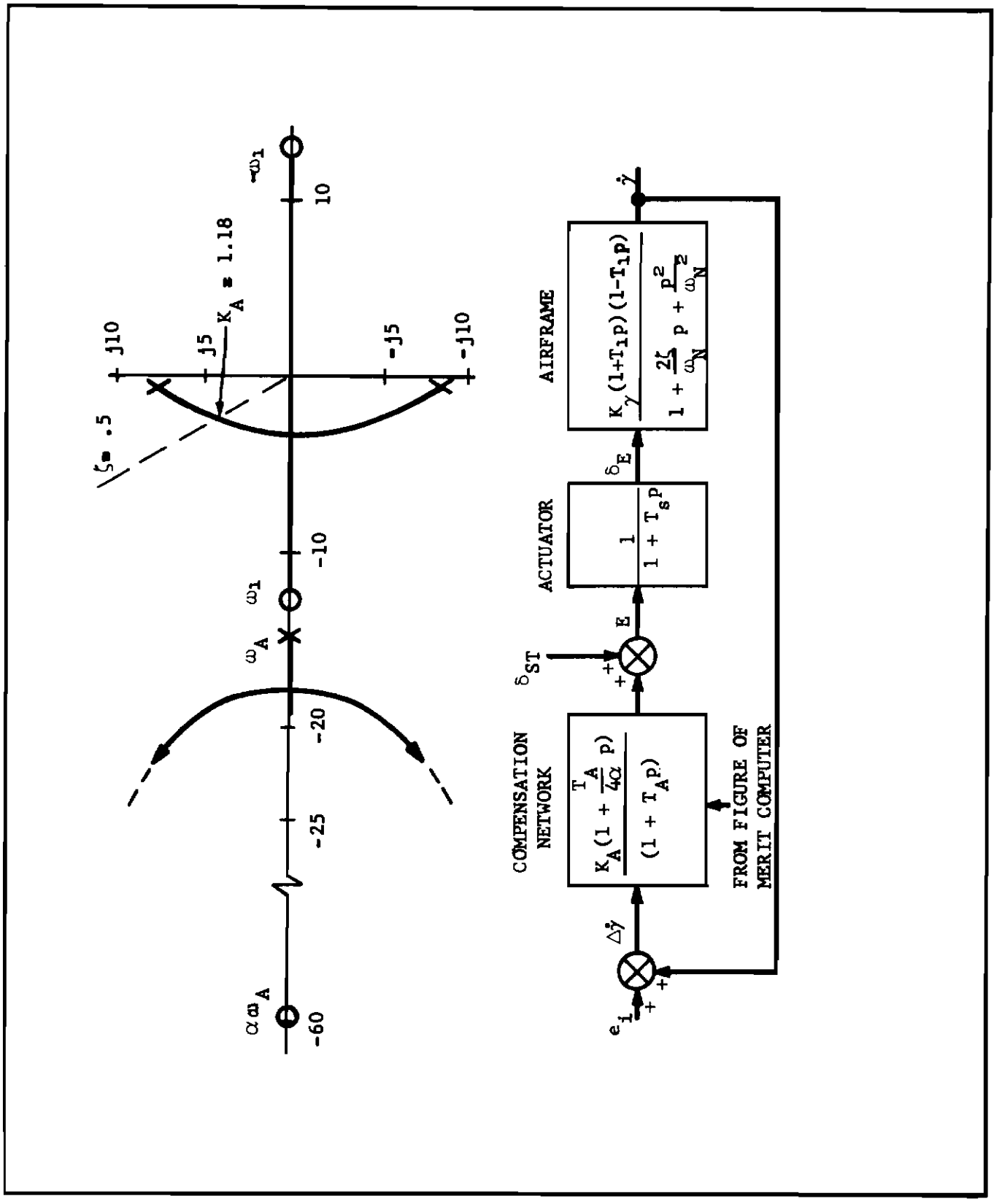

FIGURE 1-3. $\dot{\gamma}$ STABILITY AUGMENTATION

SECTION 2

THEORETICAL DISCUSSION

2.1 CROSSCORRELATOR THEORY

When a linear system is excited with a random input, the system output and the input will be correlated to an extent that depends in part upon the nature of the system. The relationship between this crosscorrelation and the system impulse response forms the theoretical basis for this method of measuring impulse response.

Consider a linear system having an impulse response $g_1(t)$, as shown in Figure 2-1, and an input $x_i(t)$ which is a stationary random variable. The system output $x_1(t)$ is easily obtained from the convolution integral as

$$x_1(t) = \int_o^\infty x_i(t - \lambda) g_1(\lambda) d\lambda \tag{2.1}$$

The crosscorrelation function of $x_1(t)$ and $x_i(t)$ is defined as an ensemble average of their product. Thus

$$\varphi_{i1}(\tau) = E[x_i(t)\ x_1(t + \tau)] \tag{2.2}$$

For stationary inputs, the sequence in which time and ensemble averages are taken can be interchanged and this leads to the result

$$\varphi_{i1}(\tau) = \int_o^\infty \varphi_{ii}(\tau - \lambda) g_1(\lambda) d\lambda \tag{2.3}$$

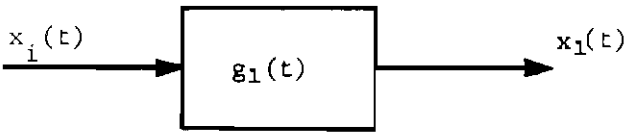

$$x_1(t) = \int_o^\infty x_i(t - \lambda)\, g_1(\lambda)\, d\lambda$$

FIGURE 2-1. LINEAR SYSTEM BEING MEASURED

where φ_{ii} is the autocorrelation function of the input.

If the input random variable is sufficiently wide-band so that it may be considered to be white noise, then

$$\varphi_{ii}(\tau) \approx N_x \, \delta(\tau) \tag{2.4}$$

and the crosscorrelator function becomes

$$\varphi_{i1}(\tau) = N_x \, g_1(\tau) \tag{2.5}$$

where N_x is the spectral density of $x_i(t)$. Hence, it is clear that determination of the system impulse response can be achieved by measuring the crosscorrelation between the system output and a suitably wide-band random input.

The crosscorrelation function can be measured, in principle, by the method shown in Figure 2-2 which involves the use of ideal delay, ideal multiplication and ideal filtering. The output of the multiplier, $x_o(t)$, has an average value which is equal to the desired crosscorrelation function at $\tau = \tau_m$. That is,

$$\bar{x}_o = E[x_i(t - \tau_m) \, x_1(t)] = \varphi_{i1}(\tau_m) \tag{2.6}$$

Hence

$$\bar{x}_o = \int_o^\infty \varphi_{ii}(\tau_m - \lambda) g_1(\lambda) \, d\lambda \tag{2.7}$$

from which it is clear that the average output is simply the convolution of the impulse response and the autocorrelation function of the input random variable.

A graphical representation of the convolution is shown in Figure 2-3. The average value $\bar{x}_o$ is simply the area under the product of the two curves shown. If the input autocorrelation function is sufficiently narrow compared to the impulse response of the system being measured, then the average value of the multiplier output will be a good indication of the value of the impulse response at $t = \tau_m$.

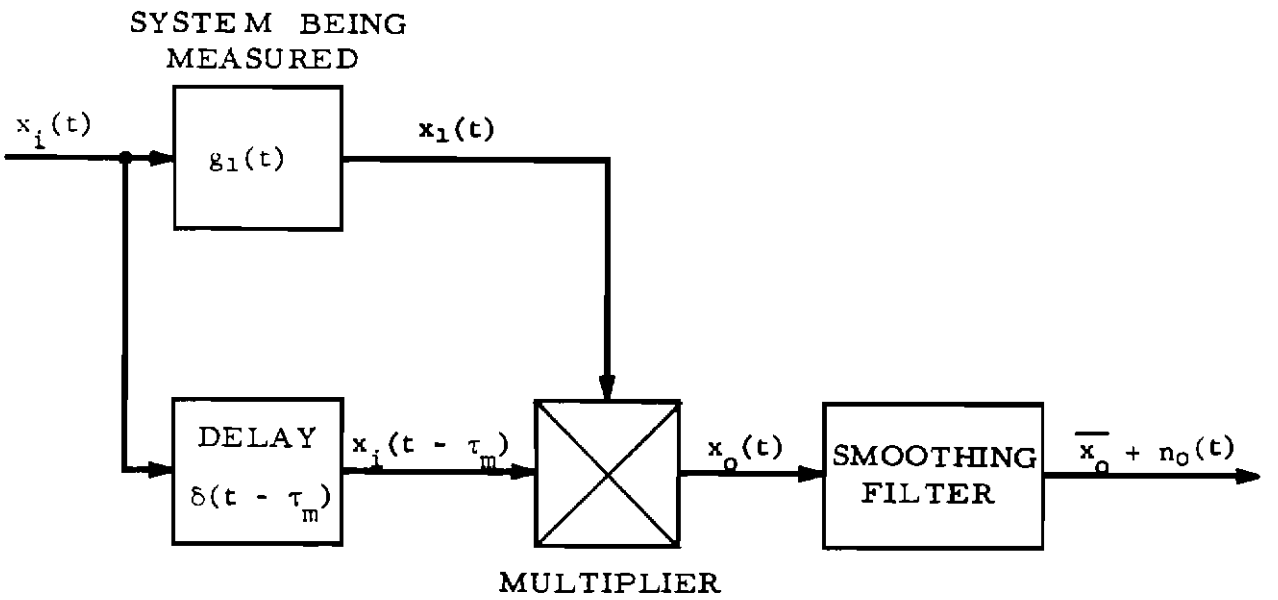

FIGURE 2-2. BASIC CORRELATOR

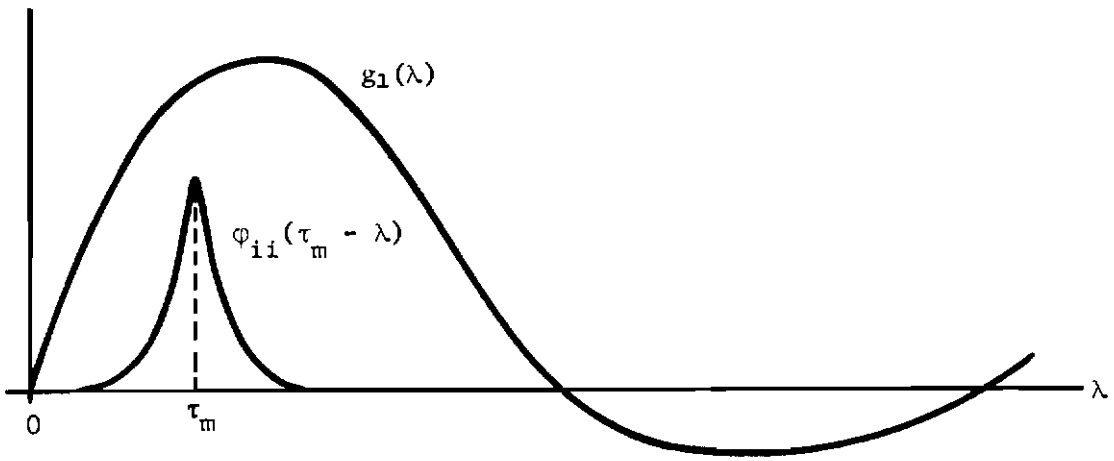

FIGURE 2-3. SHOWING THE CONVOLUTION REQUIRED TO OBTAIN $\bar{x}_o$

Obviously, if the impulse response is to be measured at several different times, it will be necessary to use different values of delay τ_m.

The multiplier output also contains a random component which must be filtered out in order to observe the desired average value. The autocorrelation function of this random component is given by

$$\varphi_{oo}(\tau) = E\left\{[x_o(t) - \bar{x}_o][x_o(t+\tau) - \bar{x}_o]\right\}$$

$$= E[x_o(t)\, x_o(t+\tau)] - (\bar{x}_o)^2 \qquad (2.8)$$

Since $x_o(t)$ can be expressed in terms of the input by

$$x_o(t) = \int_o^\infty x_i(t - \tau_m)\, x_i(t - \lambda) g_1(\lambda) d\lambda \qquad (2.9)$$

the output autocorrelation function can be written as

$$\varphi_{oo}(\tau) = \int_o^\infty d\lambda_1 \int_o^\infty E[x_i(t - \tau_m)x_i(t + \tau - \tau_m)x_i(t - \lambda_1)x_i(t + \tau - \lambda_2)]$$

$$g_1(\lambda_1) g_1(\lambda_2) d\lambda_2 - (\bar{x}_o)^2 \qquad (2.10)$$

The fourth product moment required in (2.10) can be evaluated only after the probability density functions for $x_i(t)$ are specified and this will be done in the following section.

Since the smoothing filter will have a bandwidth small compared to that of the noise out of the multiplier, it is sufficient to find the spectral density of this noise at very low frequencies only. In particular, the spectral density at zero frequency is simply

$$N_o(0) = \int_{-\infty}^{\infty} \varphi_{oo}(\tau) d\tau \qquad (2.11)$$

If the spectral density is assumed to be flat over the bandwidth of

the smoothing filter then the mean square value of the output noise becomes

$$\sigma_o^2 = 2B_2 N_o(0) \tag{2.12}$$

where B_2 is the equivalent noise bandwidth of the smoothing filter in cycles per second. A convenient measure of the goodness of filtering is the signal-to-noise ratio which may be defined as

$$z_o = \frac{(\bar{x}_o)^2}{\sigma_o^2} = \frac{(\bar{x}_o)^2}{2B_2 N_o(0)} \tag{2.13}$$

This may also be expressed in terms of smoothing time, or settling time, as

$$z_o = T \frac{(\bar{x}_o)^2}{N_o(0)} \tag{2.14}$$

in which the smoothing time

$$T = \frac{1}{2B_2} \tag{2.15}$$

has been taken arbitrarily as the time between substantially independent samples of the output noise.

In addition to the response to $x_i(t)$, the output of the system being measured will also contain responses to command inputs and to external disturbances. So far as the measurement of impulse response is concerned, these contributions represent more noise and may be considered as occurring at the output of the system as shown in Figure 2-4.

The component of multiplier output due to external noise only is simply

$$x_n(t) = x_i(t - \tau_m)\, n_1(t) \tag{2.16}$$

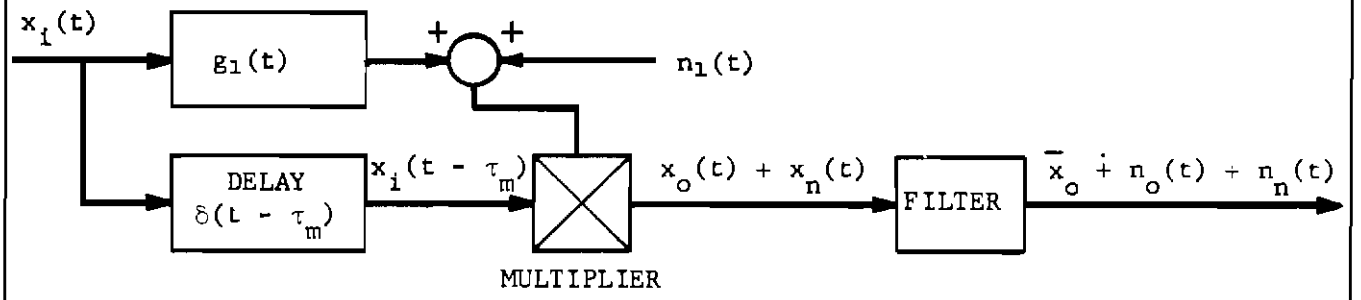

FIGURE 2-4. SYSTEM ASSUMED FOR CONSIDERING EXTERNAL DISTURBANCES

Since x_1 and n_1 are statistically independent, the autocorrelation function of x_n is just the product of the autocorrelation functions of the two factors. Thus,

$$\varphi_{nn}(\tau) = \varphi_{ii}(\tau)\ \varphi_{nn_1}(\tau) \tag{2.17}$$

where φ_{nn_1} is the autocorrelation function of n_1.

The spectral density at zero frequency for this component of noise is

$$N_n(0) = \int_{-\infty}^{\infty} \varphi_{ii}(\tau)\ \varphi_{nn_1}(\tau)\,d\tau \tag{2.18}$$

and the mean square value at the output of the smoothing filter is

$$\sigma_n^2 = 2B_2\ N_n(0) \tag{2.19}$$

2.2 SYSTEM EXCITATION

The results presented thus far have been completely general in that the nature of the excitation input, $x_1(t)$, has not been specified and can, in fact, be any stationary random process. From the standpoint of ease in mathematical analysis, the assumption that $x_1(t)$ is normally distributed would be highly desirable. However, considerable simplification of hardware, particularly in the delay and multiplication, can be achieved by using an input which has only two states (that is, binary noise). Although there are many different types of binary noise which might be considered, only two will be discussed here.

The first type, which might be called random-interval binary noise, is illustrated in Figure 2-5(a). In this case, the transitions from one state to the other occur independently and the number of such transitions in a long interval is Poisson distributed. These conditions are very nearly fulfilled by a flip-flop circuit operating on pulses from a Geiger counter exposed to a radioactive sample.

If the average number of transitions per second is β, then it can be shown that the autocorrelation function of the random-

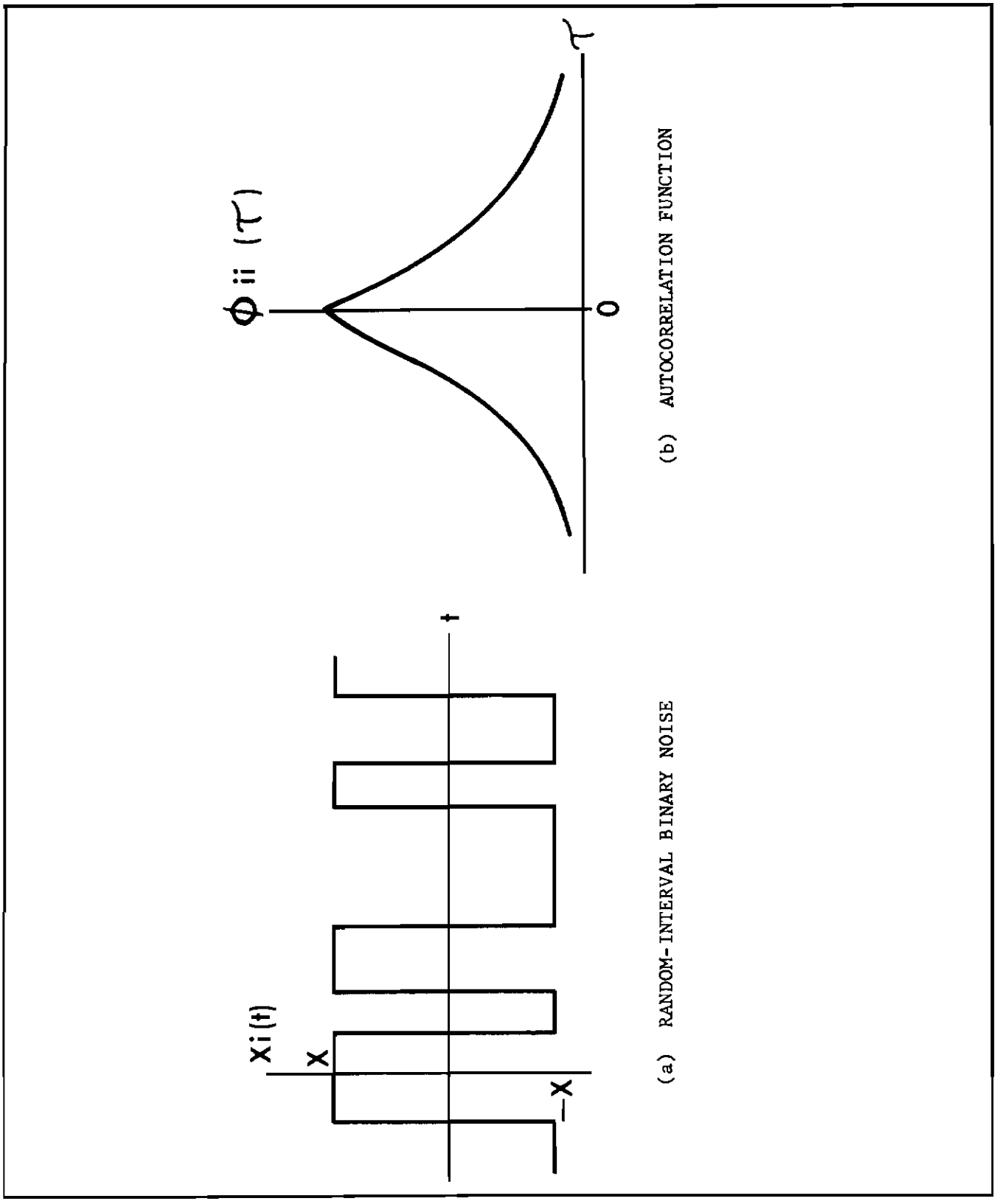

FIGURE 2-5

interval binary noise is

$$\varphi_{ii}(\tau) = X^2 \epsilon^{-2\beta|\tau|} \tag{2.20}$$

where $\pm$ X are the permitted values of $x_i(t)$. This autocorrelation function is shown in Figure 2-5(b).

The second type, which will be called discrete-interval binary noise, is illustrated in Figure 2-6(a). In this case the times at which transitions can occur are explicitly specified and the state for the succeeding interval is chosen independently of the state in any preceding interval. This type of binary noise might be generated by sampling a very wide band noise source every t_1 seconds and setting $x_1 = X$ if the sample is positive or $x_1 = -X$ if the sample is negative.

If the minimum interval width is t_1 seconds, the autocorrelation function of discrete-interval binary noise is given by

$$\varphi_{ii}(\tau) = X^2\left[1 - \frac{|\tau|}{t_1}\right] \qquad -t_1 < \tau < t_1$$

$$= 0 \qquad |\tau| > t_1 \tag{2.21}$$

This autocorrelation function is shown in Figure 2-6(b).

In the discussion of the above two types of binary noise it has been assumed that the input noise sample is of infinite duration. However, there are both practical and theoretical advantages in using an input noise sample of finite length and repeating it periodically. In the first place, the noise sample can be stored in some device which produces the delay and thus eliminates the need for a noise generator. Secondly, the filtering problem becomes easier because the average value can be extracted perfectly (in the absence of external noise) by integrating the multiplier output for exactly one period.

In considering the effect of the periodicity on the measurement of impulse response, it should be recalled that a periodic function has an autocorrelation function which is also periodic with the same period. Thus, if an ideal sample of discrete-interval binary

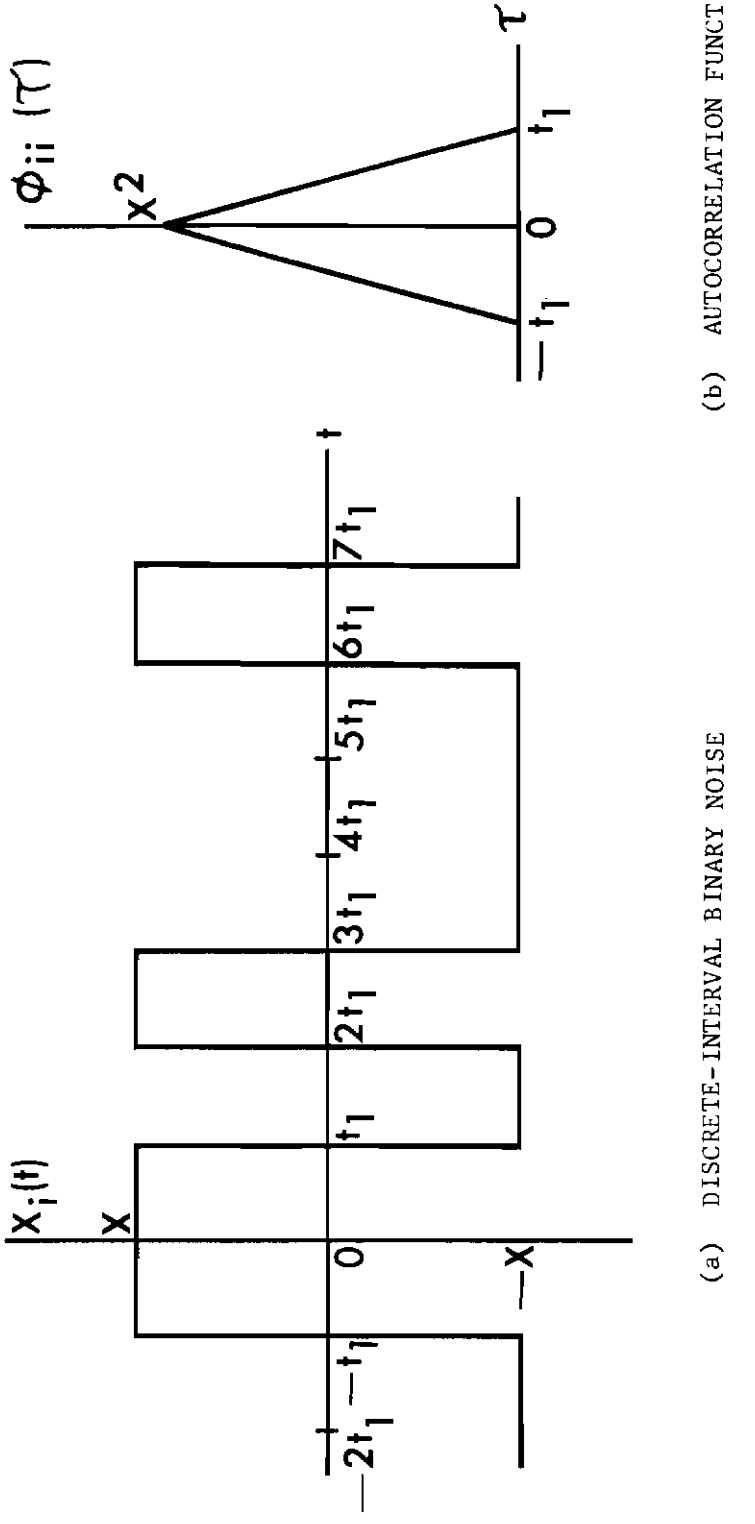

FIGURE 2-6

noise, of length Nt_1, is repeated periodically, the resulting autocorrelation function will be as shown in Figure 2-7(a). When this autocorrelation function is convolved with $g_1(t)$ in order to obtain the average multiplier output as was discussed previously, it is clear that the periodicity will have practically no effect if Nt_1 is greater than the length of the significant part of the impulse response.

One problem which does arise, however, is that of selecting an ideal noise sample. If a sample is selected at random, its autocorrelation function may differ greatly from that of the ideal sample unless Nt_1 is made quite large. This variation is a result of the statistics of a given finite length sample differing appreciably from the statistics of the ensemble. It is possible, of course, to try a large number of finite length samples until one is found which is satisfactory, but a more desirable approach would be to synthesize a noise sample having specified characteristics. Such a synthesis procedure is not available in general, but it is found for some special cases of discrete-interval binary noise.

In particular, if N, the number of discrete intervals in one period, is a prime number, it is possible to synthesize a noise sample whose autocorrelation function is of the form shown in Figure 2-7(b). Hence, if N is large (say, greater than 100) this autocorrelation function is nearly as good as that of the ideal sample. Since prime numbers are fairly evenly distributed, there is usually little difficulty in finding one close enough to the desired sample length to be useable. The synthesis procedure consists of applying some of the concepts of number theory to obtain a precise specification of the state of the random variable in every interval throughout the period. The calculation required can be easily programmed for a digital computer so there is no difficulty in obtaining noise samples for even very large values of N.

2.3 THE FILTERING PROBLEM

As has been discussed previously, the purpose of the smoothing filter is to reduce the random component of the multiplier output to a value that is sufficiently small so that the average component can be accurately observed. The computation required tc determine if this objective can be achieved started with the evaluation of the autocorrelation function of the multiplier output as given in (2.10) and this in turn requires the evaluation of the fourth product moment of the input excitation.

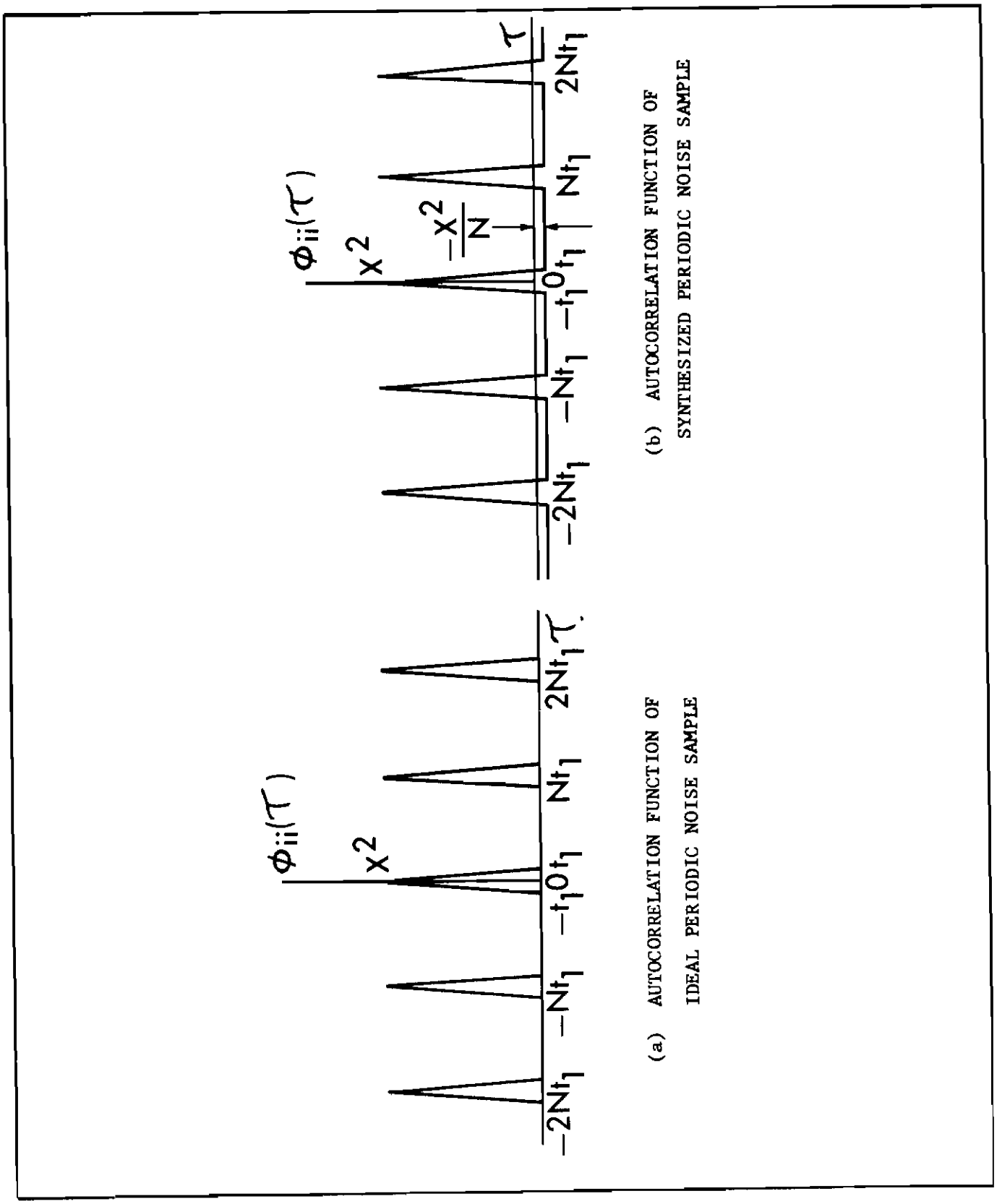

(a) AUTOCORRELATION FUNCTION OF IDEAL PERIODIC NOISE SAMPLE

(b) AUTOCORRELATION FUNCTION OF SYNTHESIZED PERIODIC NOISE SAMPLE

FIGURE 2-7

For the case of random-interval binary noise it is possible to show that the fourth product moment is given in general by

$$E[x_i(t_1)x_i(t_2)x_i(t_3)x_i(t_4)] = \varphi_{ii}(t_2 - t_1)\varphi_{ii}(t_4 - t_3) \qquad (2.22)$$

when the time instants are ordered; that is, when

$$t_4 > t_3 > t_2 > t_1$$

Thus, the evaluation of (2.10) requires breaking the plane of integration into a number of separate regions in which the variables are ordered and then using the appropriate fourth product moment for each. In addition, if the excitation noise is assumed to be very wide-band compared to the system bandwidth so that the approximation

$$\varphi_{ii}(\tau) = X^2 \epsilon^{-2\beta|\tau|} \approx \frac{X^2}{\beta}\delta(\tau) \qquad (2.23)$$

is valid, then the output autocorrelation function becomes

$$\varphi_{oo}(\tau) = \frac{X^4}{\beta^2}\left[g_1(\tau_m + \tau)g_1(\tau_m - \tau) + \delta(\tau)\int_o^{\tau_m - \tau} g_1(\lambda)g_1(\lambda+\tau)\,d\lambda\right.$$

$$\left. + \delta(\tau)\int_{\tau_m}^{\infty} g_1(\lambda)g_1(\lambda + \tau)\,d\lambda\right] \qquad (2.24)$$

From (2.11) the spectral density at zero frequency is simply

$$N_o(0) = \int_{-\infty}^{\infty} \varphi_{oo}(\tau)\,d\tau = \frac{X^4}{\beta^2}\left[\int_{-\infty}^{\infty} g_1(\tau_m + \tau)g_1(\tau_m - \tau)\,d\tau + \int_o^{\infty} g_1^2(\lambda)\,d\lambda\right] \qquad (2.25)$$

which is seen to be a function of the delay time τ_m. By application of the Schwarz inequality it is easy to show that the first integral of (2.25) can never exceed the second for any value of τ_m so that the spectral density is bounded by

$$N_o(0) \leq \frac{2X^4}{\beta^2}\left[\int_o^{\infty} g_1^2(\lambda)\,d\lambda\right] \qquad (2.26)$$

The situation is considerably different for the case of periodically repeated samples of discrete-interval binary noise. If the system being measured does not change with time, then the component of multiplier output due to excitation will also be a periodic function of time and its spectral density will contain only discrete components at the fundamental frequency and all higher order harmonics. Hence, the average value can be extracted perfectly by any filter which has zero transmission at these discrete frequencies and the smoothing time need not be greater than one period. If the system does change with time, however, the multiplier output will not be exactly periodic and some residual noise will appear at the output of the smoothing filter. Under most circumstances this noise will be small compared to that which would be obtained with non-periodic excitation.

The use of periodic excitation does nothing to alleviate the difficulty of smoothing the output noise due to external disturbances and this may often be the most important contribution. If the wideband approximation to the input autocorrelation function (2.23) is used, the low frequency spectral density of the multiplier output is obtained from (2.18) as

$$N_n(0) = \frac{X^2}{\beta} \varphi_{nn_1}(0) = \frac{X^2}{\beta} \sigma_1^2 \tag{2.27}$$

where σ_1^2 is the mean square value of the external disturbance at the output of the system being measured.

It is now possible to write a lower bound for the signal-to-noise ratio at the output of a smoothing filter having an equivalent smoothing time of T seconds under the assumption of non-periodic, wide-band excitation and the presence of external disturbances. This is

$$z_o \geq \frac{T(\bar{x}_o)^2}{N_o(0) + N_n(0)} = \frac{T \frac{X^4}{\beta^2} g_1^2(\tau_m)}{\frac{2X^4}{\beta^2} \int_o^\infty g_1^2(\lambda)\, d\lambda + \frac{X^2}{\beta} \sigma_1^2} \tag{2.28}$$

A more compact expression can be obtained by writing (2.28) in terms of the ratio of mean square excitation to mean square external disturbance at the output of the system being measured. This ratio, which is

$$z_1 = \frac{\frac{X^2}{\beta} \int_o^\infty g_1^2(\lambda)\, d\lambda}{\sigma_1^2} \tag{2.29}$$

gives a direct comparison of the relative importance of excitation and external disturbance on the system response. In terms of this ratio (2.28) becomes

$$z_o \geqslant T \frac{g_1^2(\tau_m)}{(2 + \frac{1}{z_1}) \int_o^\infty g_1^2(\lambda)\, d\lambda} \tag{2.30}$$

If the excitation is periodic, and if T is greater than one period, then the 2 in the denominator of (2.30) can be omitted. This assumes that a filter for the periodic component is used in addition to a more conventional smoothing filter for the external noise.

As an indication of the orders of magnitude involved here, assume that the system being measured is second-order with an impulse response of

$$g_1(t) = \frac{\omega_1}{\sqrt{1 - \zeta_1^2}} \epsilon^{-\zeta_1 \omega_1 t} \sin \omega_1 \sqrt{1 - \zeta_1^2}\, t \tag{2.31}$$

The value of $g_1(\tau_m)$ will, of course, depend upon the value of τ_m being considered but its maximum is very nearly

$$\text{Max}[g_1(\tau_m)] \approx \frac{\omega_1}{\sqrt{3}} \tag{2.32}$$

when $\zeta_1 = 0.5$. Likewise

$$\int_o^\infty g_1^2(\lambda)\, d\lambda = \frac{1}{2} \omega_1 \tag{2.33}$$

under the same conditions. The curves of Figure 2-8 indicate the relation among the various parameters for this special case. For periodic excitation the period is taken to be 5 seconds.

The discussion of filters so far has assumed that linear filters will be used. Since the statistics of the noise are not Gaussian it is reasonable to inquire if a nonlinear filter might not produce better results. The situation has been examined as a problem in statistical estimation in order to determine the best that might reasonably be expected without explicitly determining the type of nonlinearity required. The results indicate that for the excitation noise only the smoothing time could be reduced at most by a factor of π in the non-periodic case and not at all in the periodic case (since integration for exactly one period is still required).

When external noise is considered the results depend upon the statistics assumed for the external disturbances. If these are taken to be Gaussian, as is usually done, then the multiplier output will have a first-order probability density function which is Gaussian and a joint probability density function which is nearly Gaussian. Under these circumstances the minimum variance estimator is nearly linear. Hence, it has been concluded that when periodic excitation is used, nonlinear filtering does not offer sufficient improvement to justify its use.

It has also been assumed so far that the parameters of the system being measured do not change with time and on this basis the signal-to-noise ratio out of the correlator can be made arbitrarily large simply by increasing the smoothing time. This assumption is unrealistic, however; in fact, the major purpose of the cross-correlation technique is to make it possible to measure changes in system parameters. It is clear, therefore, that the maximum smoothing times that can be tolerated will depend in some way upon the maximum rate at which the system parameters will change.

If the system impulse response is considered to be time-varying, it may be designated as $g_1(t, \lambda)$ which is defined as the response at time t to an impulse applied at time λ. When non-periodic binary excitation is applied, the signal component out of the multiplier is easily shown to be

$$\bar{x}_o(t) = \frac{X^2}{\beta} g_1(t, t - \tau_m) \qquad (2.34)$$

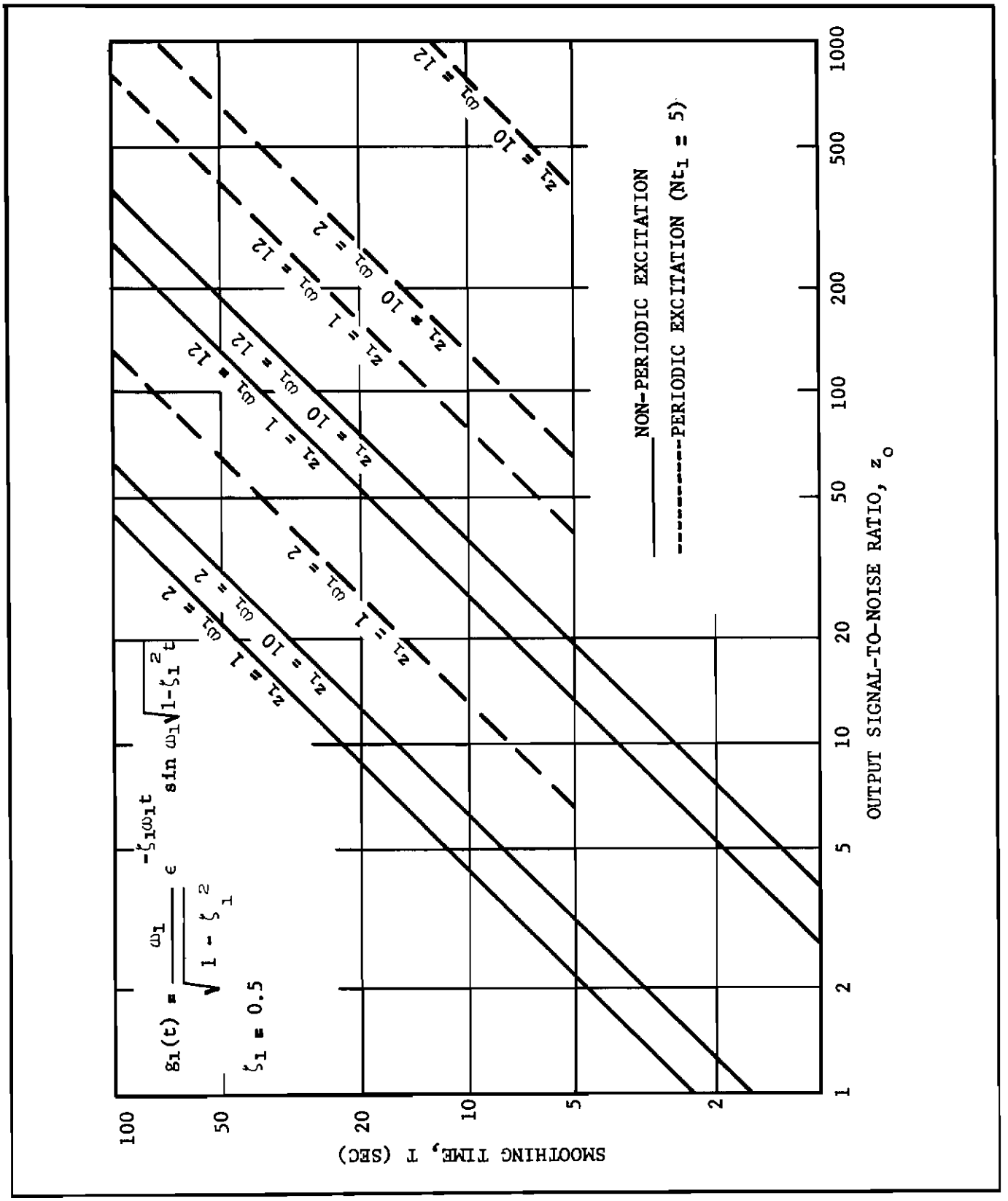

FIGURE 2-8. SMOOTHING TIME VS. SIGNAL-TO-NOISE-RATIO

which is also a function of time. The smoothing time of the filter must therefore be small enough to reproduce $\bar{x}_o(t)$ with any specified degree of accuracy. It is difficult to draw general conclusions here but any specific time variation of the impulse response can be investigated in detail.

It may also be noted from (2.34) that there is a lag of τ_m between the time a change in the system occurs and the time that it may be fully observed in $\bar{x}_o(t)$. As a rough illustration of this, Figure 2-9 shows a hypothetical situation in which the impulse response at τ_m changes from one constant value to another constant value at t=0. The average value of correlator output does not completely reach its new value until $t = \tau_m$.

2.4 MEASUREMENT OF SYSTEM DAMPING

It has been demonstrated that the crosscorrelation procedure makes it possible to measure the impulse response of a system at a number of discrete points. A possible application of this procedure is to determine how well the system is damped, but in order to do this it is first necessary to relate some characteristic of the impulse response to the system damping. A characteristic which appears to be suitable for this purpose is the ratio of the positive area of the impulse response to the negative area.

In the case of a second-order system such as defined by (2.31), it can be shown that the area ratio is

$$R = \left|\frac{A_+}{A_-}\right| = \epsilon^{\frac{\pi\zeta_1}{\sqrt{1-\zeta_1^2}}} \tag{2.35}$$

where A_+ is the positive area of $g_1(t)$, A_- is the negative area, and ζ_1 is the damping ratio. It is clear, therefore, that R is a monotonic function for ζ_1 and is independent of the natural frequency ω_1. Thus, a measured value of area ratio uniquely determines the system damping ratio.

For higher-order systems there is no such simple mathematical relation between area ratio and system damping but their physical relationship is essentially the same. This fact may be made more

evident by recalling that the step response of a linear system is simply the area under the impulse response. Hence, the overshoot on the step response is directly related to the amount by which the positive area exceeds the net area which can, in turn, be related to the area ratio.

If the correlator is to be used as a component of an adaptive system which is to control damping, then it is desirable to create an error signal which is zero at the desired value of damping and has opposite polarity on either side of this. Such an error signal, which will be designated as the figure of merit, can be formed by multiplying the negative area of the impulse response by the desired area ratio and adding it to the positive area. Thus,

$$F_m = A_+ + R_o A_- \tag{2.36}$$

where R_o is the area ratio corresponding to the desired system damping.

In the present case the entire impulse response is not available but only a finite set of discrete values. Hence, the appropriate areas can be approximated by multiplying the known ordinates of $g_1(t)$ by the spacing between ordinates and adding. On this basis, the figure of merit becomes

$$F_m = \sum_{m=1}^{M} A_m \, g_1(\tau_m) \tag{2.37}$$

where M is the number of correlators being used and

$$A_m = a_m \qquad g_1(\tau_m) > 0$$

$$= R_o a_m \qquad g_1(\tau_m) < 0$$

$$a_m = \frac{1}{2} (\tau_{m+1} - \tau_{m-1})$$

In actuality, however, the time values of $g_1(\tau_m)$ are not available but only a set of random variables having average values

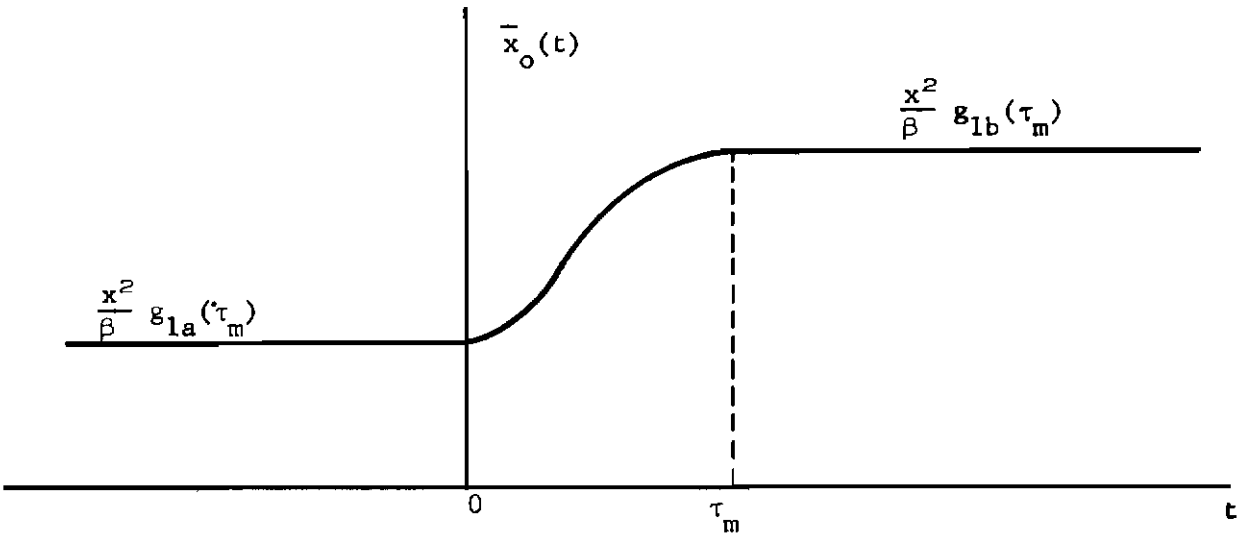

FIGURE 2-9. CHANGE IN OUTPUT CAUSED BY A STEP CHANGE IN IMPULSE RESPONSE

proportional to $g_1(\tau_m)$. Hence, the computed figure of merit will also be a random variable and subject to several kinds of errors. In the first place, the output of any correlator is to be multiplied by R_o or not depending upon whether that output is negative or positive. For those channels in which the average value is small, the output will fluctuate across zero. Because all negative values are multiplied by R_o (which may be about 6), the resulting average will be biased negatively by an amount which depends upon the magnitude of noise. Because of this bias the figure of merit will go through zero at a different value of system damping than it should.

Furthermore, the variations in figure of merit due to the noise may be quite large because the noise out of all the correlators is being added. In addition, for those channels in which $g_1(\tau_m)$ is negative, the noise is being multiplied by R_o.

Two steps can be taken to reduce the above errors in figure of merit. First the weighting factor of R_o can be applied to a given channel on the basis of the sign of $g_1(\tau_m)$ rather than the sign of the correlator output. This can be done by making an independent measurement of natural frequency as discussed in the next section. Secondly, those channels in which the average value is small can be completely eliminated from the computation of figure of merit on the grounds that they contribute little to the result anyway. This procedure eliminates the noise and bias errors that these channels would otherwise produce.

When the parameters of the system being measured change with time an additional error in the figure of merit is produced by the delay in the correlator. As was discussed in the preceding section, there is a lag of τ_m in any channel between the time a parameter change occurs and the time its effect is fully apparent in the correlator output. The resulting lag in the figure of merit will depend upon how the delays for the various channels are distributed. If the delays are spaced approximately exponentially (closer spacing at small delays), a step change in system damping might result in a change in figure of merit as shown in Figure 2-10. It is assumed in this sketch that the system damping changed at $t = 0$ from some value less than the desired value to a greater value.

When the correlator and figure of merit computer are used as part of a closed-loop system to control damping, the resulting errors in damping arise primarily from noise and bias errors in the

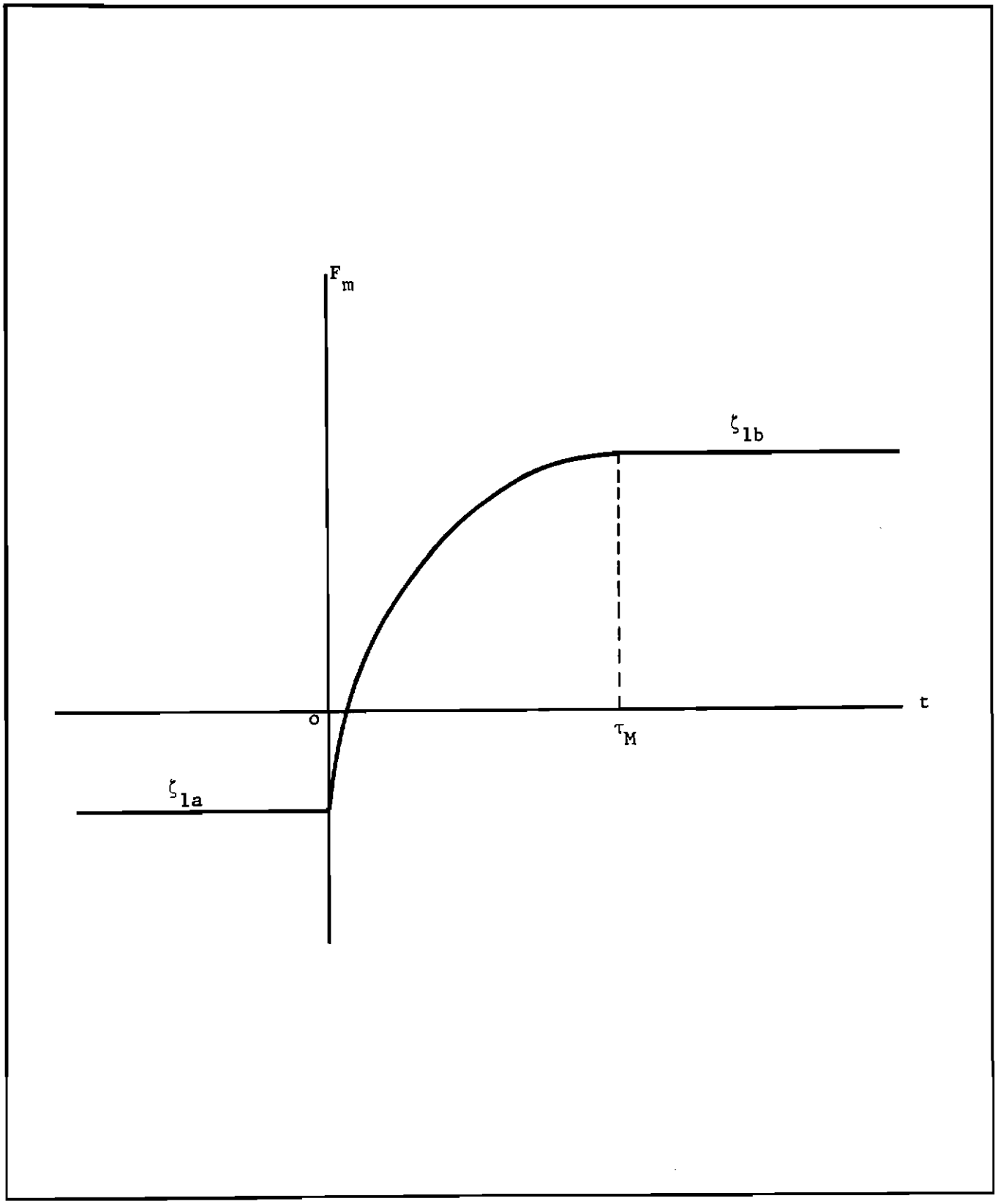

FIGURE 2-10. CHANGE IN FIGURE OF MERIT CAUSED BY A STEP CHANGE IN DAMPING

figure of merit and from the lag introduced by the correlators. The latter can be approximately compensated by a linear network but this increases the error due to noise. The final compensation of the closed-loop system therefore represents a three-way compromise among peak error, velocity error and noise error when the system parameters are assumed to change at some maximum rate.

2.5 MEASUREMENT OF NATURAL FREQUENCY

It may be desirable to measure the natural frequency of a system either for the purpose of controlling it or for the purpose of improving the computation of figure of merit as has just been discussed. It is possible, of course, to determine the natural frequency from a knowledge of the damping and the time that the impulse response goes through its first zero. However, it is of interest to note that an independent measurement is also possible.

Consider a crosscorrelator of the form shown in Figure 2-11 and note that this differs from the original correlator only in that a differentiator has been added. It can be shown that the average value of the multiplier output is

$$\bar{x}_o = \frac{X^2}{\beta} \frac{d\, g_1(\tau)}{d\tau} \tag{2.38}$$

when the excitation is non-periodic binary noise. For a second-order system of the form described by (2.31), and for no delay ($\tau = 0$), this becomes

$$\bar{x}_o = \frac{X^2}{\beta} \omega_1^2 \tag{2.39}$$

from which it is clear that the natural frequency can be obtained independently of the damping.

For higher order systems the initial slope of the impulse response is zero and the measurement $\tau = 0$ gives no information. However, by introducing a small delay, it is again possible to obtain the natural frequency. For example, in a third-order system with a real pole at $-\alpha$ and a small delay of τ_1, the average output becomes

$$\bar{x}_o \approx \frac{X^2}{\beta} \alpha\, \tau_1\, \omega_1^2 \tag{2.40}$$

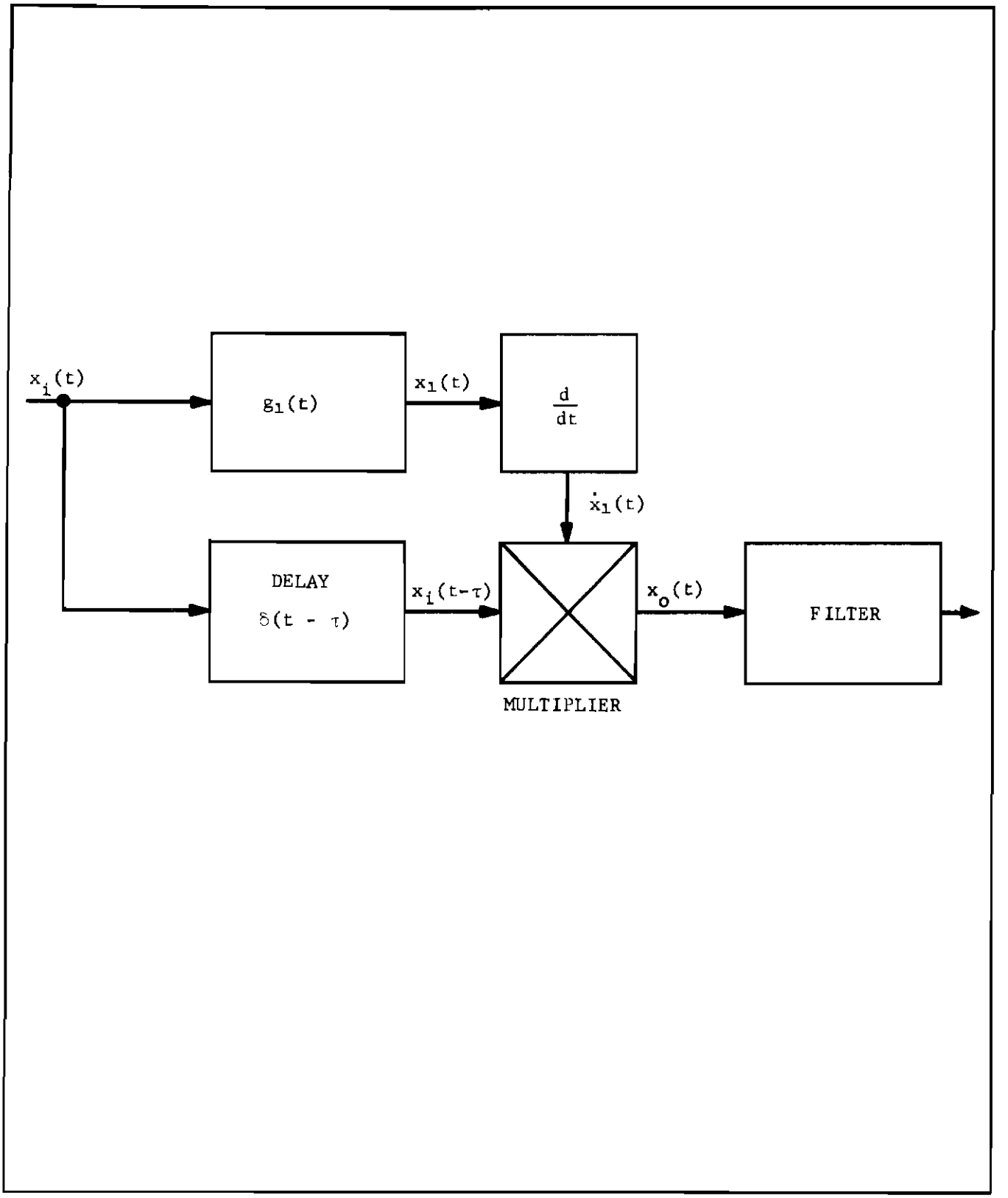

FIGURE 2-11. SYSTEM FOR MEASURING NATURAL FREQUENCY

This result is still independent of the damping ζ_1 but does depend upon α which may or may not be known.

Essentially the same results can be obtained by introducing the differentiation before the system being measured or before or after the delay. In all cases, however, the signal-to-noise ratio out of the correlator is poorer than without differentiation.

SECTION 3

CROSSCORRELATOR MECHANIZATION

Several approaches to the mechanization of the cross-correlator have been investigated, including the use of analog, digital, and combined analog-digital techniques. Figure 3-1 is a flow diagram of the mathematical operations to be performed. These include noise generation, time delay generation, multiplication, and integration with respect to time.

3.1 NOISE GENERATION

Complexity of the mechanization is determined to a great extent by the waveform generated by the random noise generator. Since there are no restrictions on the statistical properties of the noise as far as the impulse response computation is concerned, there are several techniques for noise generation available to us. Of these, binary noise appears to offer the most advantages as far as simplifying the system mechanization. The resulting system employs a combination of analog and digital techniques.

A typical sample of binary noise is shown in Figure 3-2. The waveform has constant amplitude but random polarity and with a Poisson distribution for the pulse lengths, ℓ. Because the design of the time delay generator is based on periodic sampling of the noise signal, it is necessary to place a lower limit on the pulse length such that no pulse occurs whose length is shorter than a.

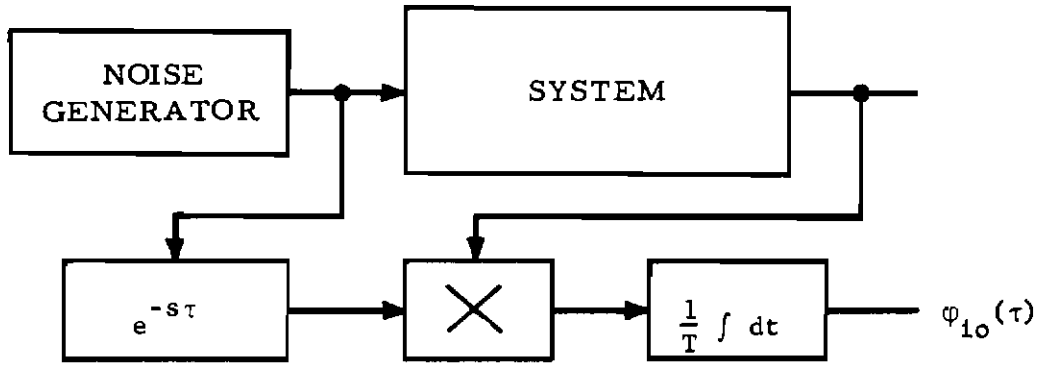

$$\varphi_{io}(\tau) = \lim_{T\to\infty} \int_{-T}^{T} \varphi_{ii}(\tau - t)\, g(t)\, dt$$

FIGURE 3-1. OPERATIONS REQUIRED TO COMPUTE CROSSCORRELATION COEFFICIENTS

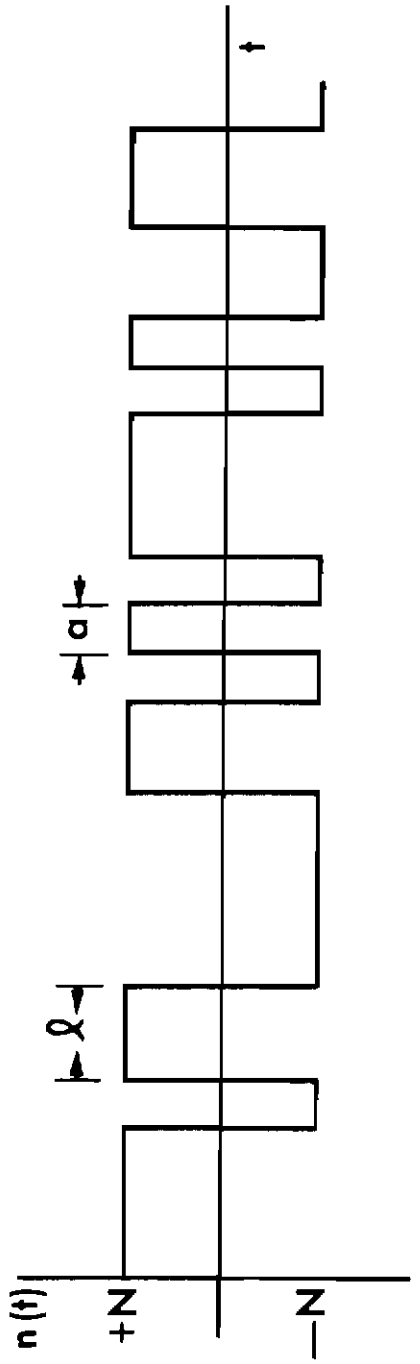

FIGURE 3-2. BINARY NOISE SAMPLE

Figure 3-3 is a block diagram of a suitable random noise generator. Randomly occurring pulses are obtained from a Geiger counter excited by a radioactive sample. These pulses are passed through a one-shot multivibrator serving as the pulse period discriminator. The one-shot insures that successive pulses in its output do not occur closer together than the minimum pulse period a. A flip-flop is triggered by the discriminated pulse train to generate the waveform shown in Figure 3-2. Bandwidth adjustments are made by varying the count rate from the Geiger counter and by varying the minimum pulse period.

An alternative to the use of a random noise generator is the employment of a recorded noise sample which is repeated over and over again. As noted earlier, such an "ideal" noise sample has some very attractive properties which make it a more desirable noise source than the random noise generator.

3.2 TIME DELAY GENERATION

Turning our attention to the time delay generator, we note that the time delay generator accepts the noise signal as an input and generates several outputs, one for each point on the system impulse response. The question arises as to how many points to compute. Certainly a sufficient number of points must be included to obtain all of the significant information available in the system response. In the systems to be evaluated with this correlator, the natural frequencies are expected to vary from 2 rad/sec to 12 rad/sec. As shown in Figure 3-4, it appears that a satisfactory approach is to compute a fixed number of points with exponential spacing between points. In this manner, we can obtain a good spread of the points in the first part of the response at both high and low frequencies. The low frequency limit establishes the requirement for the maximum time delay at approximately four seconds. Experimental evidence indicates that 12 points on the impulse response will give adequte information. Hence the time delay generator must produce 13 outputs, one for the system excitation and 12 delayed signals, with delays from 0.01 seconds to 4.0 seconds spaced exponentially.

A pure time delay of the order of several seconds without significant distortion is usually difficult to obtain. However, the binary characteristic of the noise signal permits us to employ some relatively simple digital techniques to obtain many seconds of delay in increments of hundredths of a second.

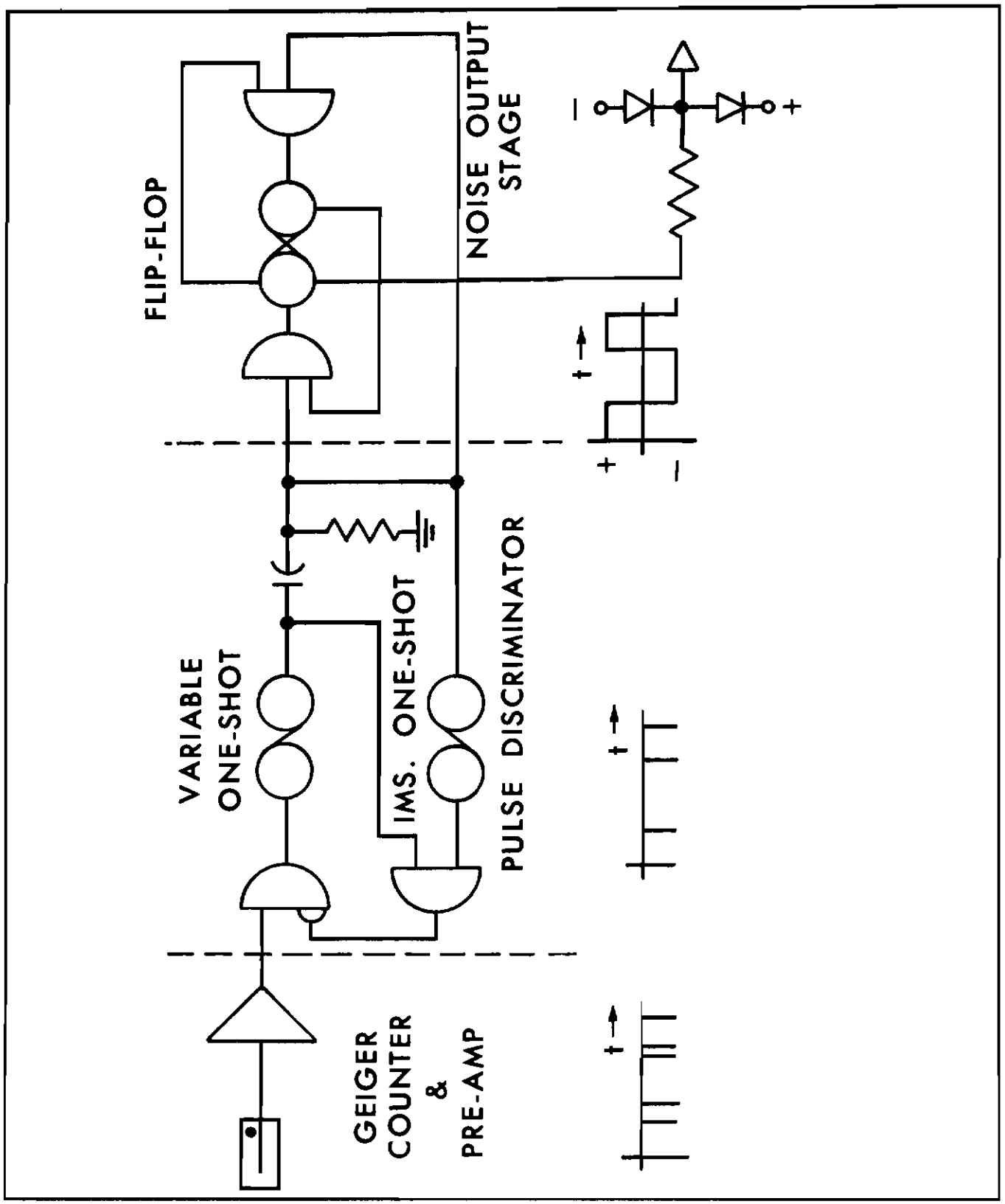

FIGURE 3-3. BLOCK DIAGRAM - RANDOM NOISE GENERATOR

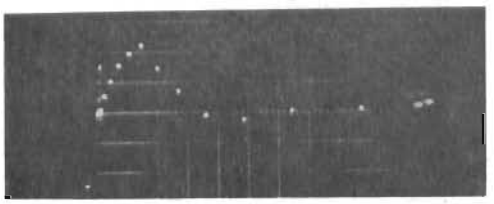

ω = 2 rad/sec. ζ = 0.4

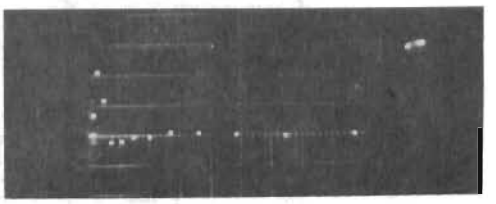

ω = 12 rad/sec ζ = 0.4

FIGURE 3-4. EXPONENTIAL SPACING OF CORRELATOR POINTS

The scheme is based on sampling the random or asynchronous input to generate a periodic or synchronous digital signal which is propagated through a shift register. The shift register is in effect a discrete delay line which can be tapped at several points. Reconstruction of the sampled noise is effected in a one-bit storage unit, a flip-flop, in the output of each channel.

3.3 MULTIPLICATION

Multiplication is also simplified by the binary character of the noise signal. The noise signal passing through the time delay generator is normalized to an amplitude of ± 1, since the digital circuits do not sense amplitude. Multiplication of the system response by ± 1 simply means that we connect either the system response or its inverse to the multiplier output. This is a simple gating operation that may be accomplished either electronically or with relays.

3.4 AVERAGING

Computation of the average value of the multiplier output completes the crosscorrelation computer. The average value is obtained by passing the multiplier output through a low pass filter consisting of one or two long time constant RC sections.

3.5 CROSSCORRELATION HARDWARE

A block diagram of this crosscorrelator is shown in Figure 3-5.

Note that one additional component appears in this diagram, specifically, the readout commutator. This is necessitated by the design of the shift register. To delay several seconds of information arriving at rates of the order of hundreds of bits per second requires a shift register of considerable capacity. For example, in the system under discussion, it is necessary to obtain ten seconds delay at an information rate of 100 bits per second. This requires a shift register with the capacity to store 1000 bits of information. A shift register of this size assembled from flip-flops or magnetic cores proves to be quite expensive, and the degree of flexibility afforded is not required. Consequently, the shift register is mechanized as a precessing circulating register on a magnetic drum. All of the information stored in the circulating register is read out during each revolution of the drum. The

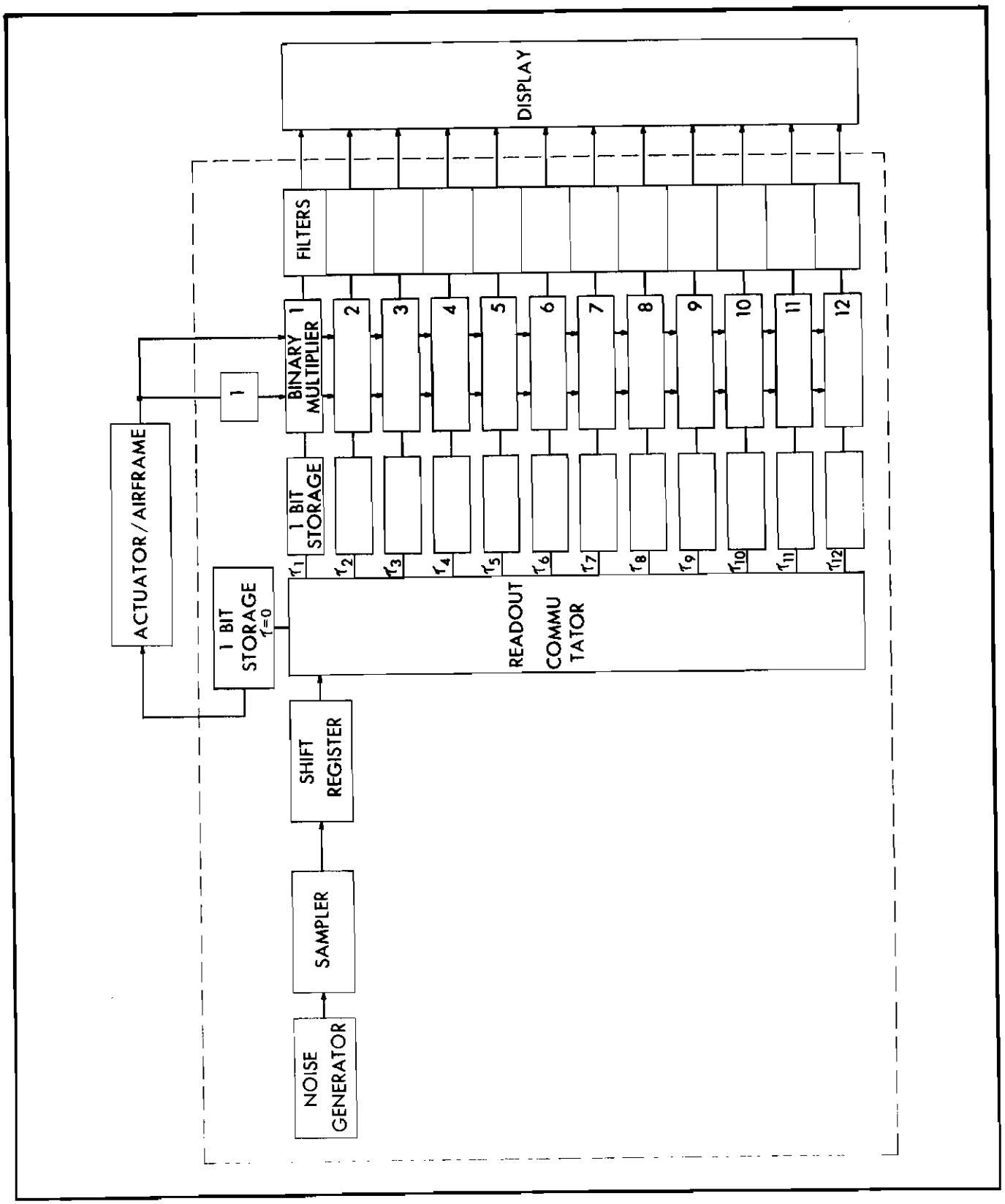

FIGURE 3-5. BLOCK DIAGRAM - CROSSCORRELATOR

readout commutator is required to distribute the proper bits to the output storage flip-flops.

Figure 3-6 is a photograph of a breadboard model of the correlator built for use with the analog computer. Figure 3-7 is a photograph of the experimental model to be flight tested this spring. Etched circuit boards and solid-state components have been employed throughout the unit. However, no attempt has been made to optimize the airborne package since the circuit boards employed were designed for a general purpose computer. Considerable saving in size and weight could be made by employing components tailored to the application.

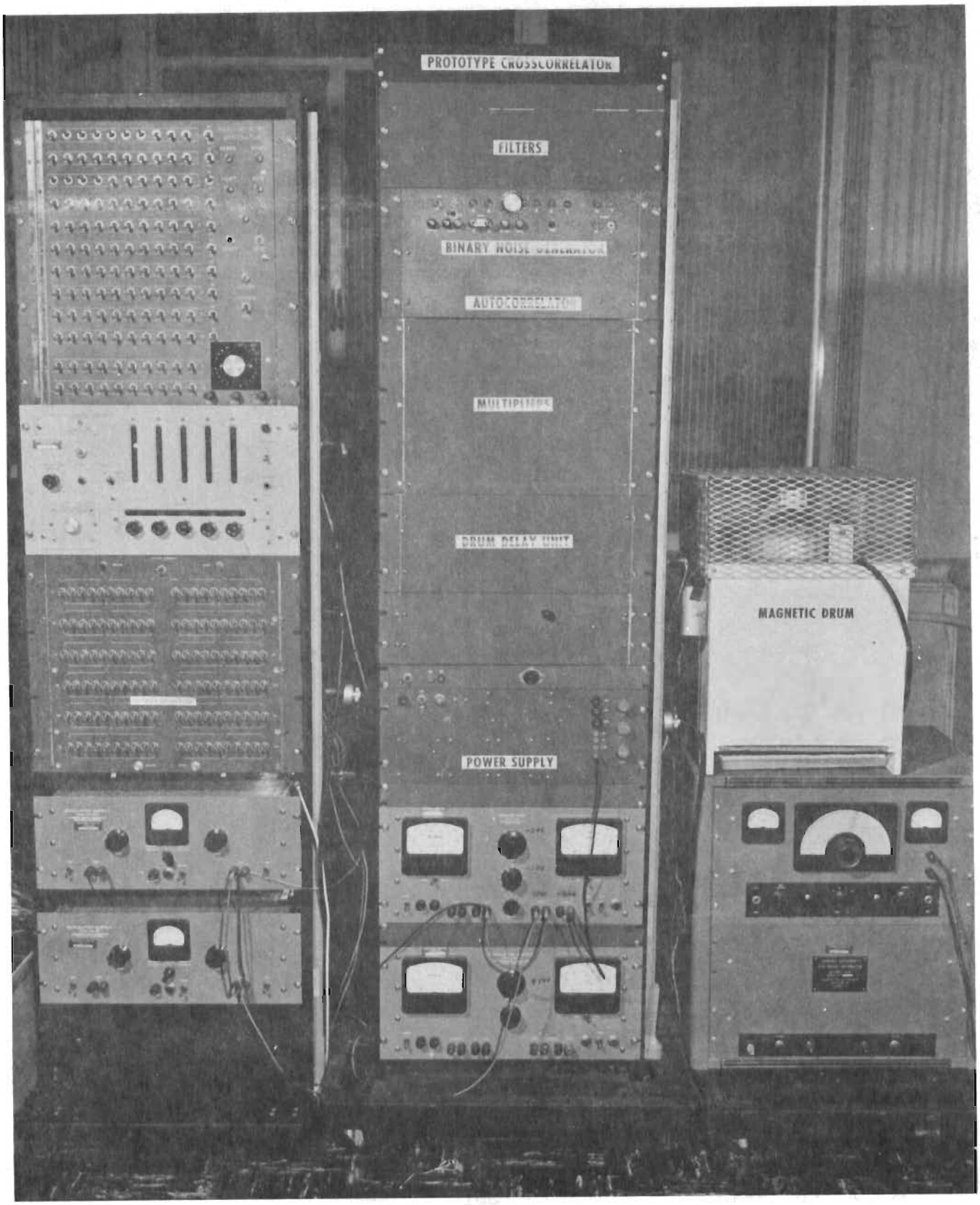

FIGURE 3-6. BREADBOARD MODEL OF CROSSCORRELATOR AND TEST EQUIPMENT

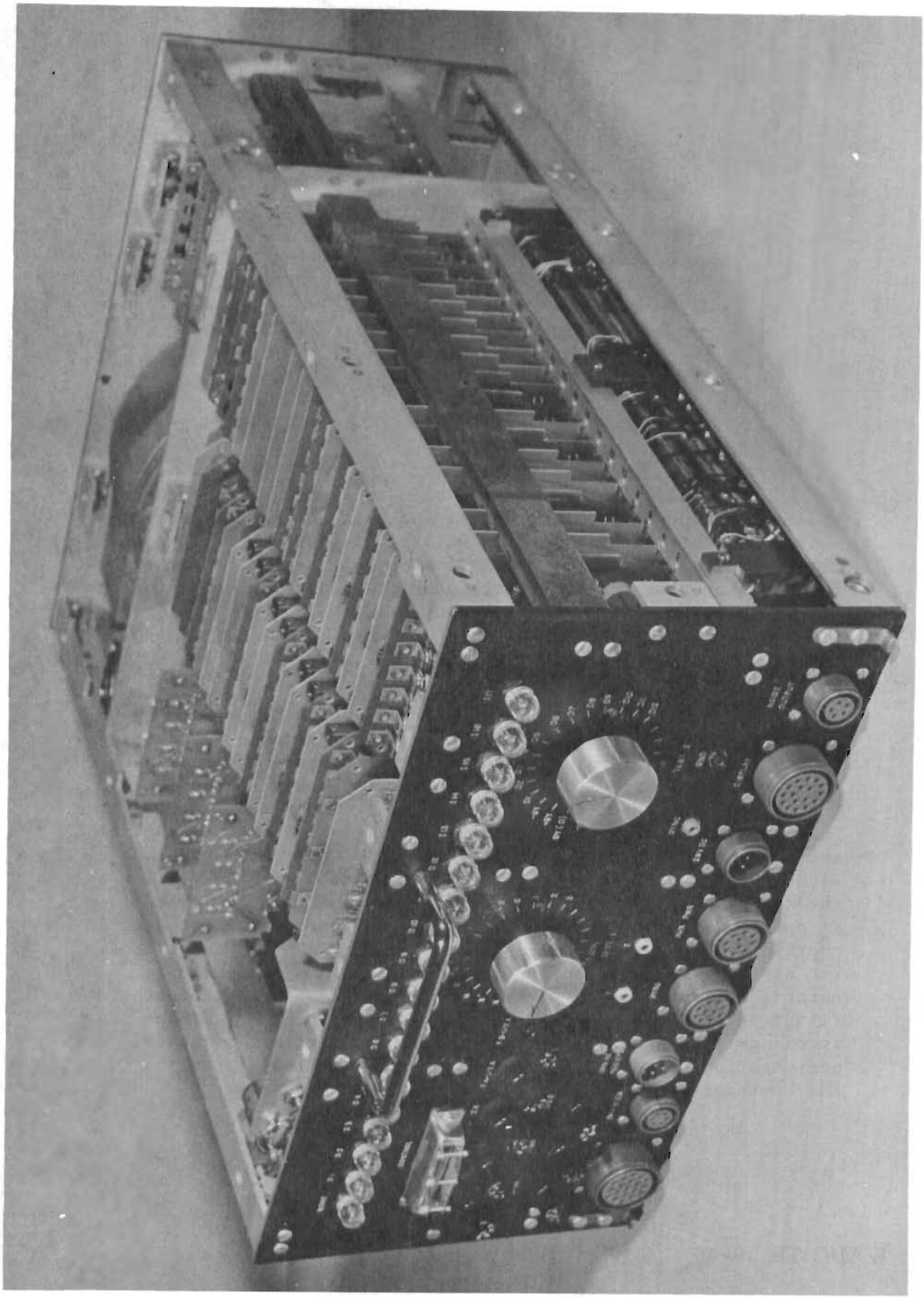

FIGURE 3-7. AIRBORNE MODEL OF CROSSCORRELATOR

SECTION 4

SIMULATION STUDIES

Simulation studies have been conducted throughout this program to support the theoretical analysis and hardware development. Several of these studies will be discussed briefly to illustrate that the Aeronutronic concept of adaptive control is feasible and that the crosscorrelator is capable of measuring the airframe response with good accuracy.

4.1 DEMONSTRATION OF ADAPTIVE PITCH DAMPER

A pitch damper with a variable compensation loop was simulated to demonstrate that adaptive control could be achieved by monitoring the impulsive response of the system. The stability augmenter chosen for this demonstration is shown in Figure 4-1. The rate of change of flight path angle $\dot{\gamma}$ is the control parameter. This type of control was chosen because of simplicity of control and the fact that the closed loop response was predominantly second order. The gain K_a and time constant T_a are controlled by the adaptive loop. The ratio of K_a to T_a is fixed at 17.5. Thus K_a and T_a can both be controlled from one shaft. The actuator is represented by a single lag with a time constant of 0.05 seconds. The airframe is represented by the short period mode with a natural frequency which varied from 2 to 12 rad/sec within the flight regime chosen. Note that the damping of the dominant roots increases with increasing gain. For the conditions simulated, the compensation network gain varied from 0.2 to 3.5 in order to keep the dominant root damping ratio at 0.5.

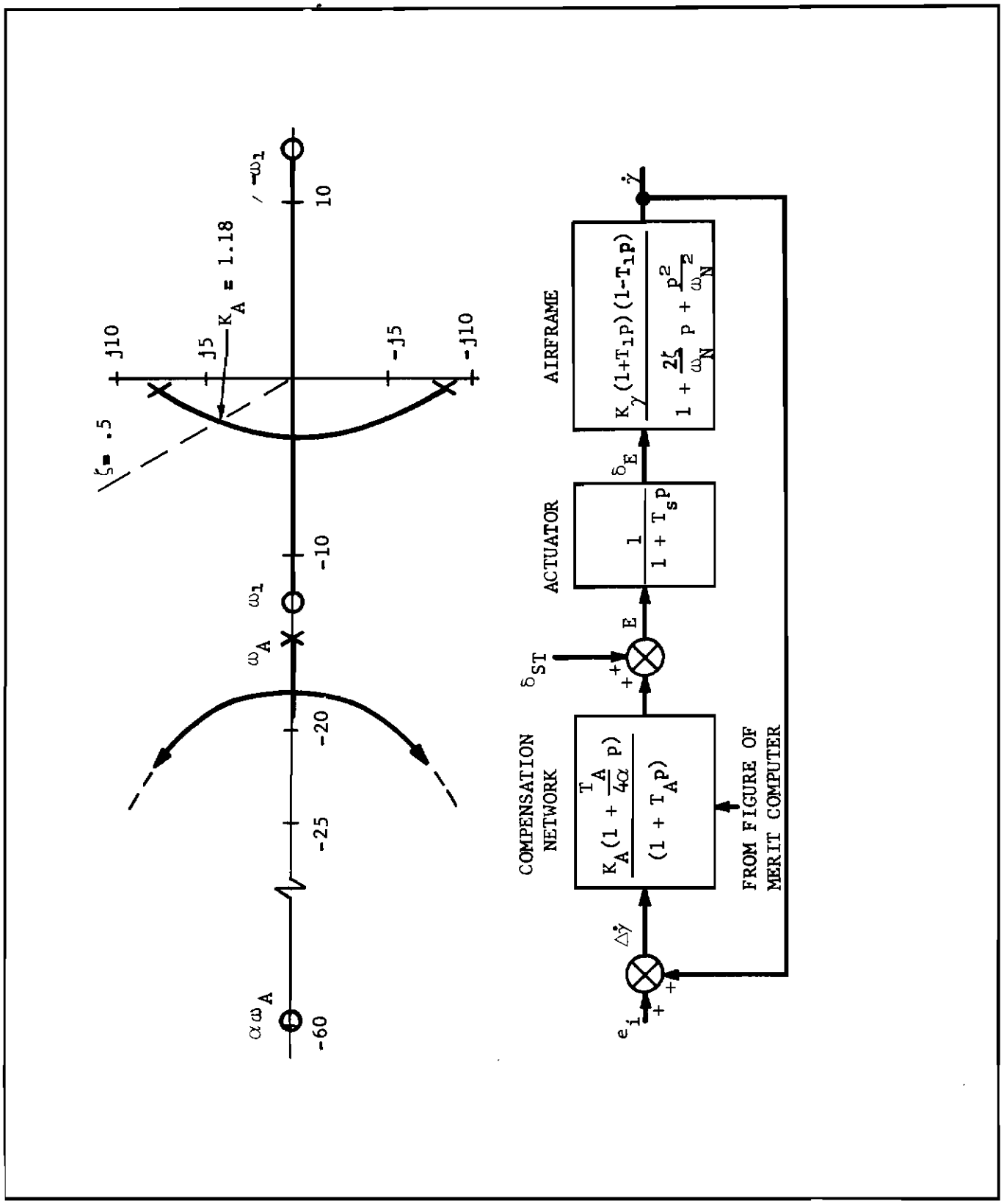

FIGURE 4-1. $\dot{\gamma}$ STABILITY AUGMENTATION

The self-adaptive system block diagram is shown in Figure 4-2. The system impulsive response is obtained by forcing the system with impulses supplied by a pulse train generator. The repetition rate of the pulses was chosen so that the system response decays to zero between successive pulses. The Figure of Merit Computer measures the system damping ratio. When the damping is greater than the desired 0.5, the F_M signal is positive and visa versa. The F_M signal is sampled at the end of each pulse period and held until the end of the following period. Just prior to the end of the following period and after sampling, the Figure of Merit Computer output is reset to zero and a new cycle begins. The Compensation Controller controls the rate of change of K_a and T_a. This rate is directly proportional to the output of the sample and hold circuit, F_{Ms}.

The system operation is actually an iteration process: Assume that initially the system is overdamped, that is, K_a and T_a are too large. When the initial impulse is applied, an overdamped response results and the Figure of Merit is positive. This signal is held during the following cycle and the Compensation Computer decreases K_a and T_a at a constant rate. This continues until the damping ratio is 0.5 and F_M is zero. Thereafter K_a and T_a track the changes in damping ratio as the aerodynamic conditions change.

The results of a climbing flight are shown in Figure 4-3. The velocity is held at Mach 1.2 while the aircraft climbs from sea level to 60,000 feet. When the compensation loop is open, a large variation in system damping is apparent. In contrast, when the compensation control loop is closed, a fairly uniform $\dot{\gamma}$ response is obtained when traversing the identical flight trajectory. Thus an adaptive pitch damper has been achieved.

4.2 CROSSCORRELATOR CAPABILITIES

The crosscorrelator is the heart of the Aeronutronic adaptive autopilot concept. If the ASI system is to function properly, the crosscorrelator must measure the impulsive response of the system continuously and accurately. Simulation techniques have been used to demonstrate that this can be accomplished.

The accuracy of the crosscorrelator was determined by cross-correlating a second order system and making twenty independent measurements of each correlation coefficient. Typical results are shown in Figures 4-4 and 4-5.

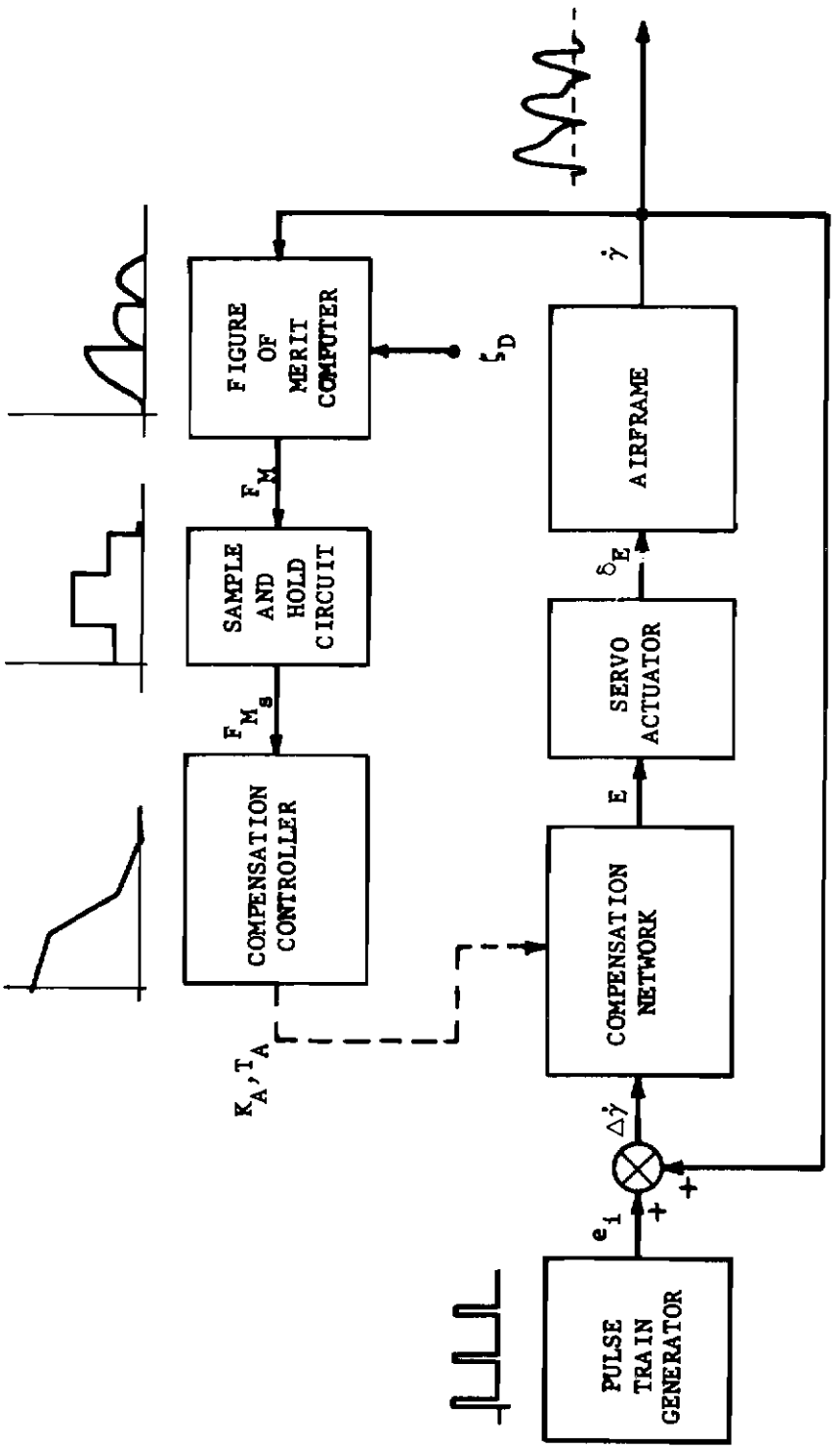

FIGURE 4-2. BLOCK DIAGRAM - IMPULSE EXCITED SOAP SYSTEM

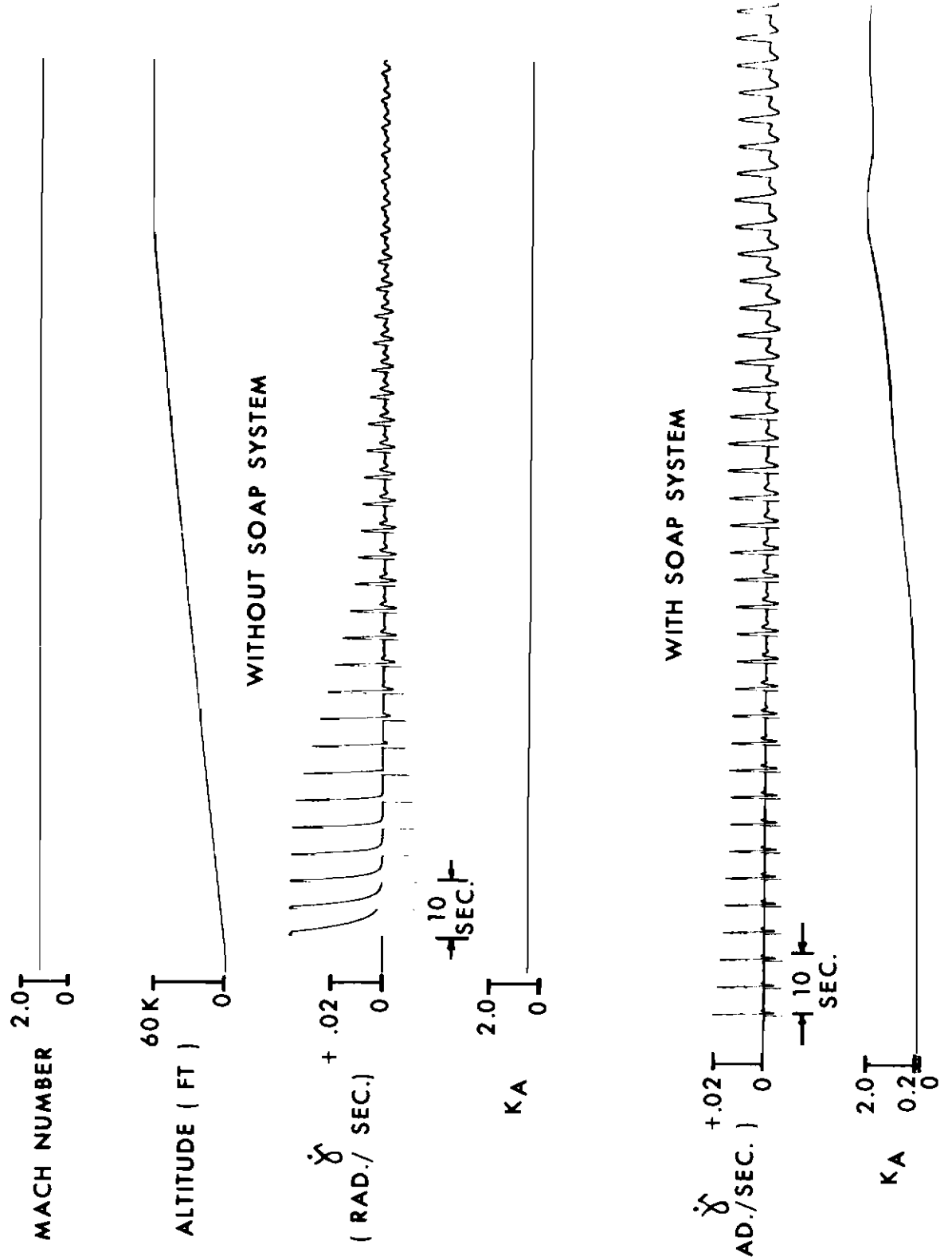

FIGURE 4-3. CLIMBING FLIGHT USING IMPULSE EXCITED SOAP SYSTEM

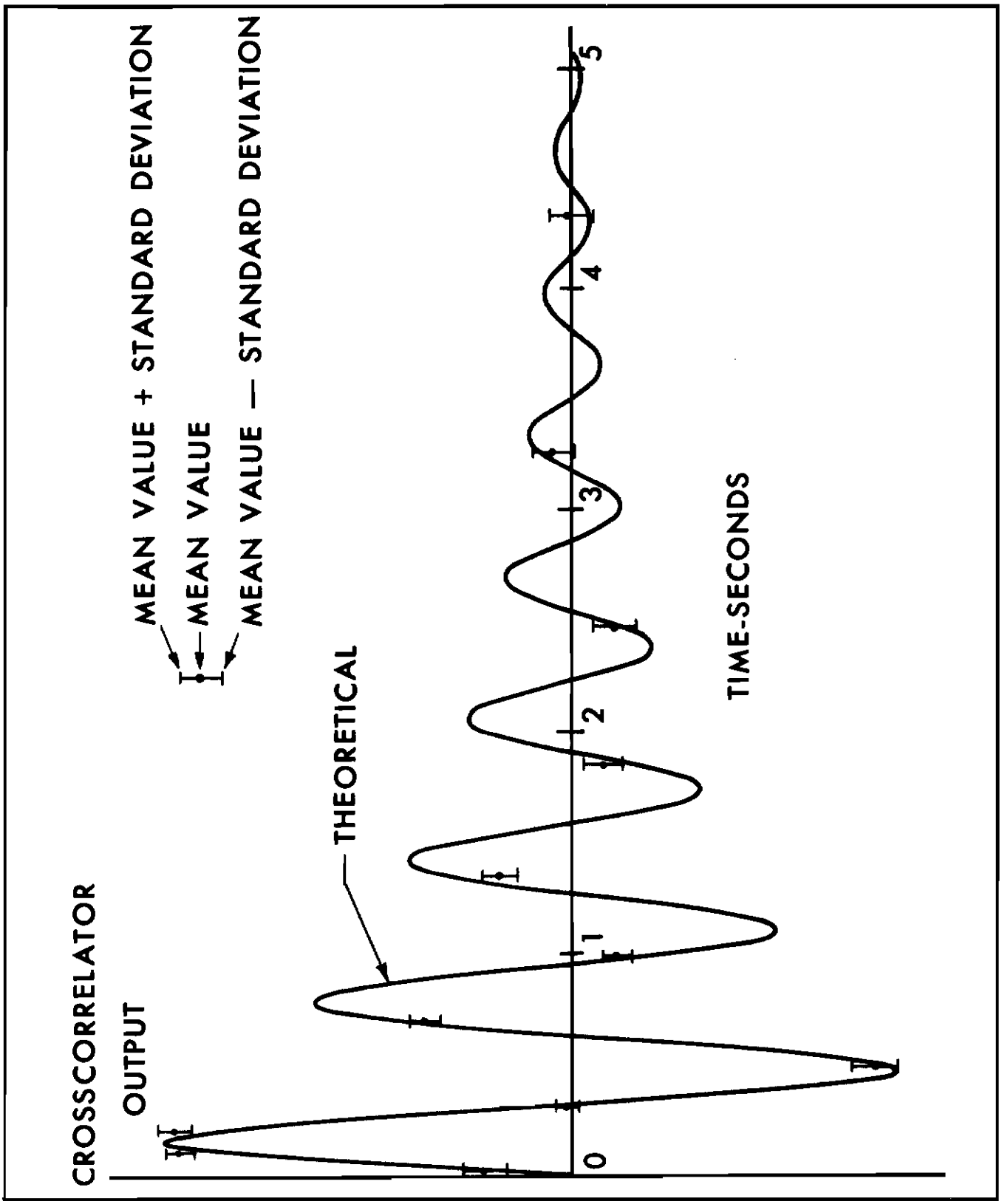

FIGURE 4-4. IMPULSE RESPONSE OF SECOND ORDER SYSTEM WITH ω_n = 10 RPS and ζ = .1

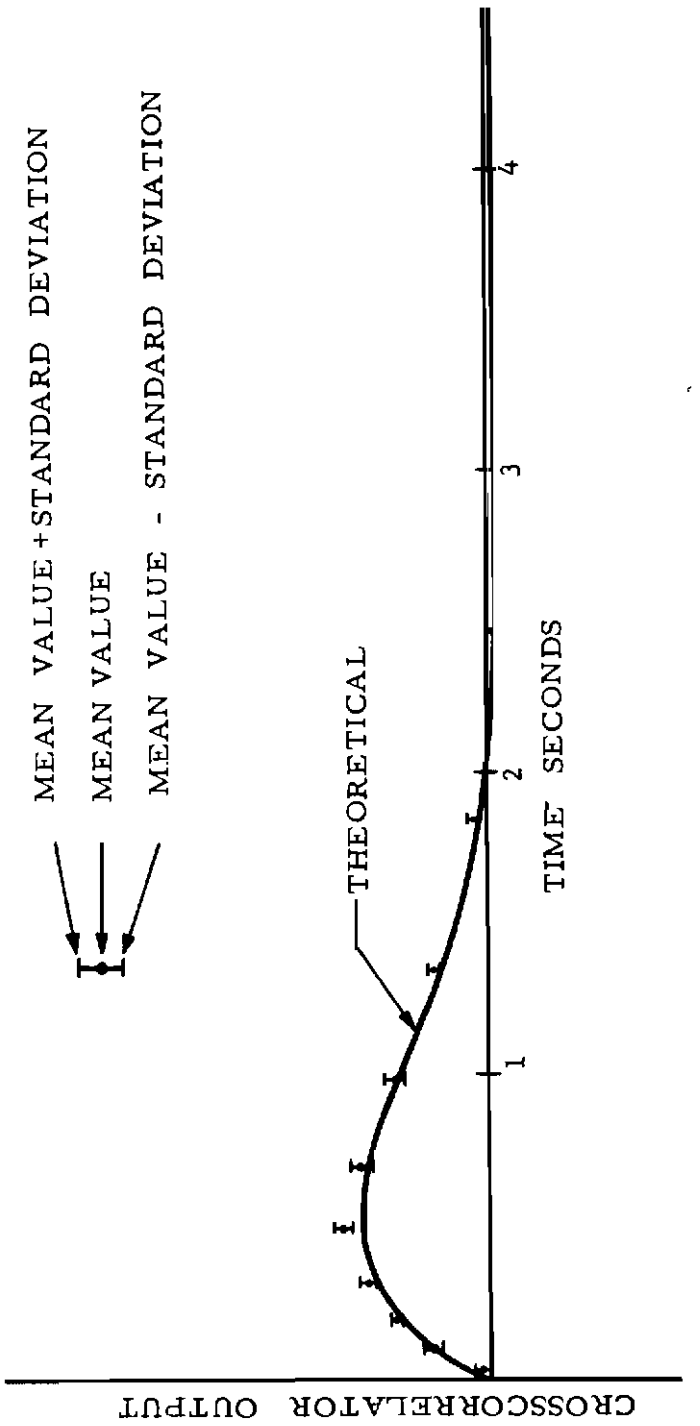

FIGURE 4-5. IMPULSE RESPONSE OF SECOND ORDER SYSTEM WITH ω_n = 2 RPS AND ζ = .7

Figure 4-4 shows the impulsive response of a second order system with a natural frequency of 10 rad/sec and a damping ratio of 0.1. The dots are the mean value of the twenty readings of each coefficient. The two bars above and below each point are plus and minus one standard deviation about each mean. Figure 4-5 is the same type of presentation but for a second order natural frequency of 2 rad/sec and a damping ratio of 0.7. The standard deviation is always less than 10 per cent of the maximum amplitude of the impulsive response and is about 5 per cent in most cases. The measured variance of the correlation coefficients is almost entirely due to the statistical nature of the correlation signal and was predicted from theory. The crosscorrelation equipment does not cause any appreciable error.

ASI is currently engaged in preparing to flight test the crosscorrelator. Studies have shown that it would be highly desirable to obtain data in the air which could be used as a check of the crosscorrelator. However, the nonlinearities of the actuator plus mechanization difficulties make it undesirable to attempt to apply impulses to the control surface and thus to obtain the impulsive response of the system. On the other hand, the airframe response to a small step input is easily mechanized. The system response can be measured by the crosscorrelation method by inserting a pure integration in series with the actuator airframe and making the integrator a part of the system. Practically this is difficult, so a low pass filter with a twenty-second time constant was substituted for the pure integration.

The crosscorrelation and the step response are compared in Figure 4-6 for the simulated pitch mode of a supersonic aircraft. The crosscorrelation coefficients have been corrected for the effect of the low pass filter which makes the coefficients with the longer delays decay toward zero. Thus the crosscorrelation technique may be used to obtain impulse or step response whichever is easiest or most desirable to measure.

The effect of nonlinear components in the autopilot system has been of some concern in studying the crosscorrelator. The effect of such nonlinearities is also important in flight testing the crosscorrelator because we wish to measure the airframe response as accurately as is possible. For the above reasons a separate study was made of the nonlinear actuator which we will have in our F-100C flight test vehicle. The characteristics of the actuator are shown in Figure 4-7.

The actuator is essentially a first order lag in closed loop form. The open loop gain N_1 is nonlinear as is shown. The result is

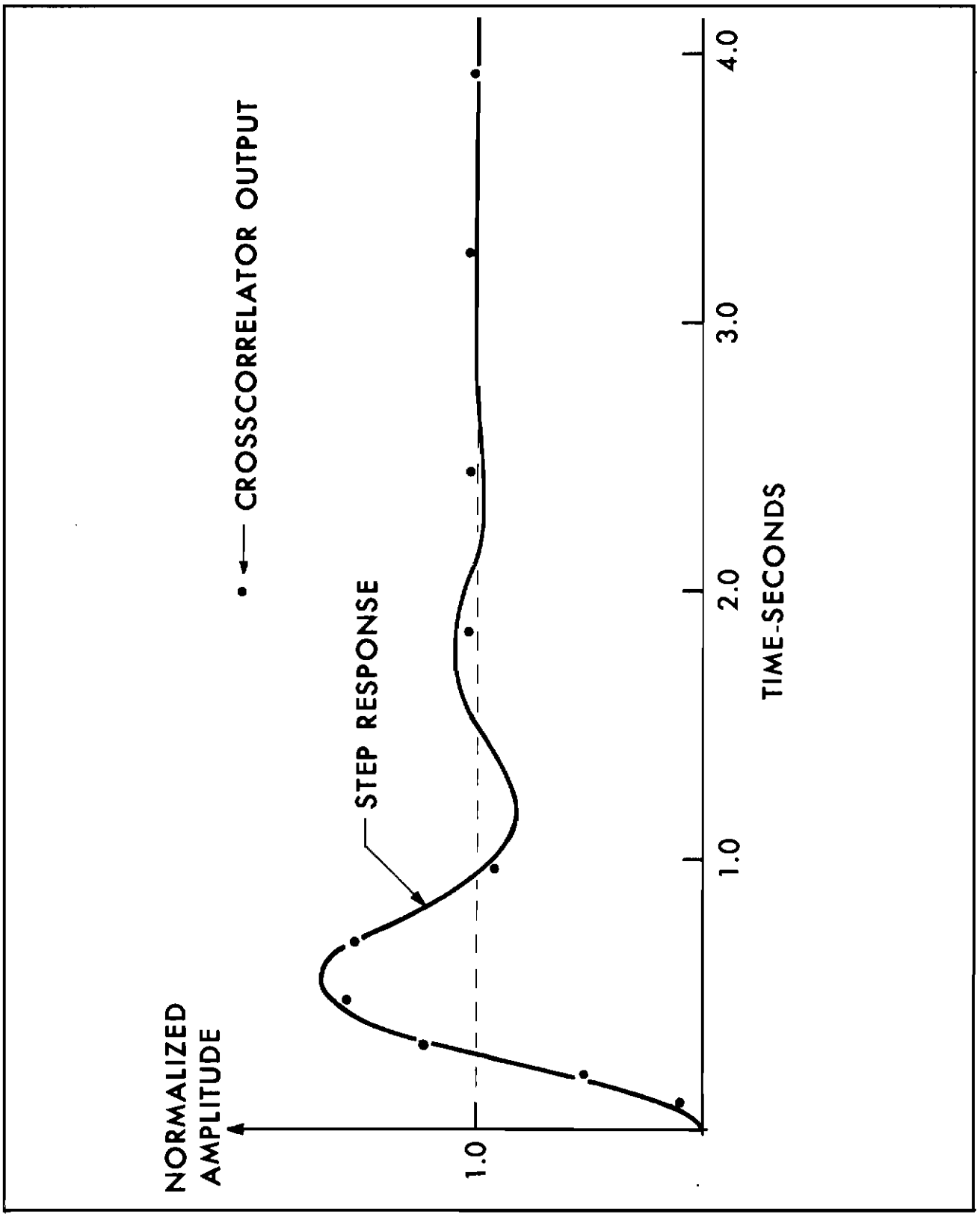

FIGURE 4-6. STEP RESPONSE OF F-100 AIRFRAME FOR LOW ALTITUDE CONDITION

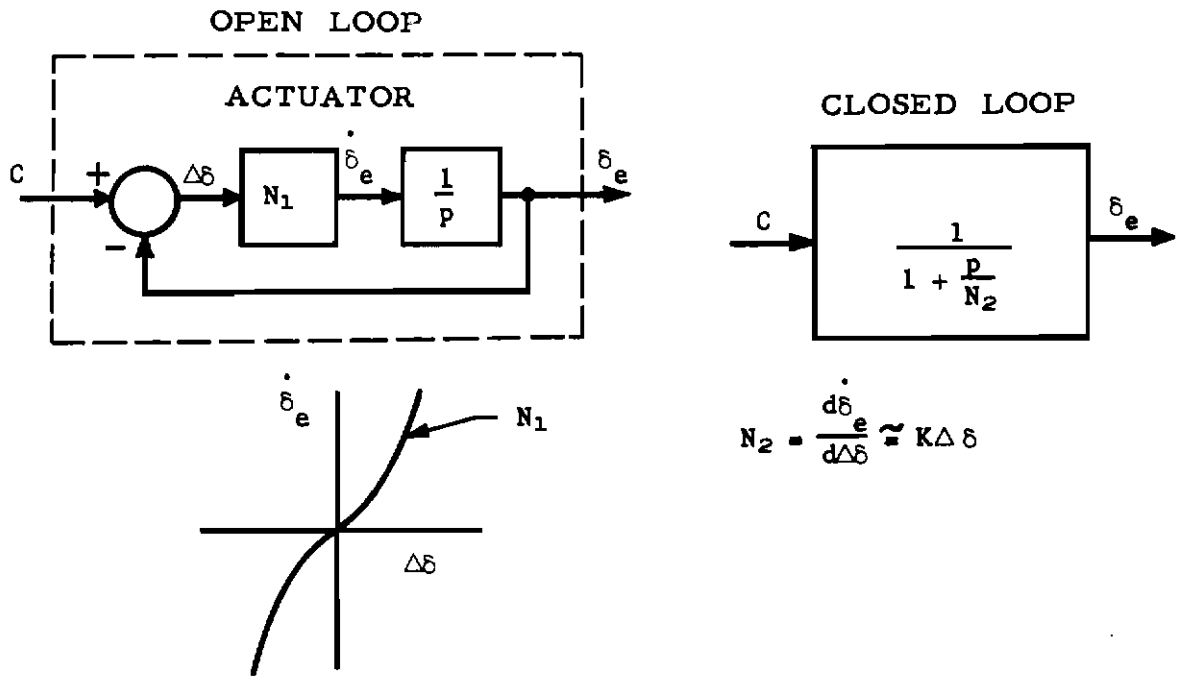

FIGURE 4-7. NONLINEAR ACTUATOR CHARACTERISTICS

that the closed loop time constant $1/N_2$ varies directly as the error $\Delta\delta$. Thus the actuator is sluggish for low level inputs and has a short response time for large inputs.

Figure 4-8 shows the crosscorrelation of the actuator for four different levels of input. Note the first order impulsive response decays faster as the input amplitude is increased. The time constant for each input amplitude was measured from the crosscorrelation coefficients and was computed from the characteristic of N_1. Figure 4-9 shows the variation in N_2 with the input amplitude C for both methods. Thus the crosscorrelator measured the nonlinear characteristic quite accurately.

The F-100C pitch damper system has been studied when backlash and dead space are present. The effect did not appreciably affect the crosscorrelation of the system. It appears that the nonlinearities encountered in the aircraft actuator will not present any problem to the crosscorrelation technique.

The use of the crosscorrelation technique was suggested by Bootan as a means of describing certain types of nonlinearities. Dr. Rideout and his group at the University of Wisconsin have been using the crosscorrelation to obtain generalized error functions for linear and nonlinear servos. It would seem that the crosscorrelation technique has considerable potential in this field.

4.3 SUMMARY

The concept of self-adaptive control by monitoring the system impulsive response has been shown to be feasible. Also the crosscorrelator has been shown to have good accuracy and to have acceptable capability in spite of nonlinearities encountered in aircraft actuators. There remains the demonstration of adaptive control with the correlator in the system. This has been done for a second order system and was reported in the technical literature*.

In the near future, the pitch damper loop will be simulated with the crosscorrelator. However, major emphasis to date has been placed upon the components of the system such as the Figure of Merit computer, the control of natural frequency, and the development of a periodic noise generator.

---

* 1958 IRE National Convention Record, Part 4 "A Self-Adjusting System for Optimum Dynamic Performance"

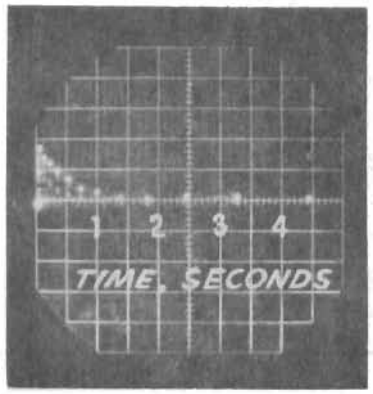

(a) INPUT AMPLITUDE 0.05 DEG.

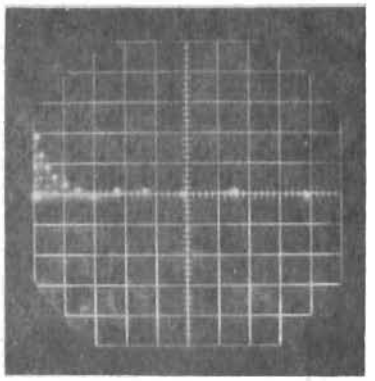

(b) INPUT AMPLITUDE 0.25 DEG.

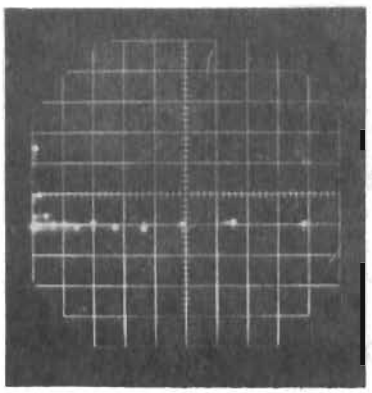

(c) INPUT AMPLITUDE 0.5 DEG.

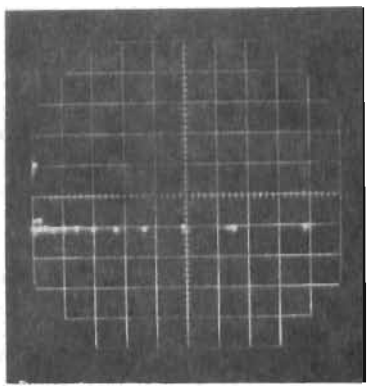

(d) INPUT AMPLITUDE 1.0 DEG.

FIGURE 4-8. CROSSCORRELATION OF NONLINEAR ACTUATOR SYSTEM

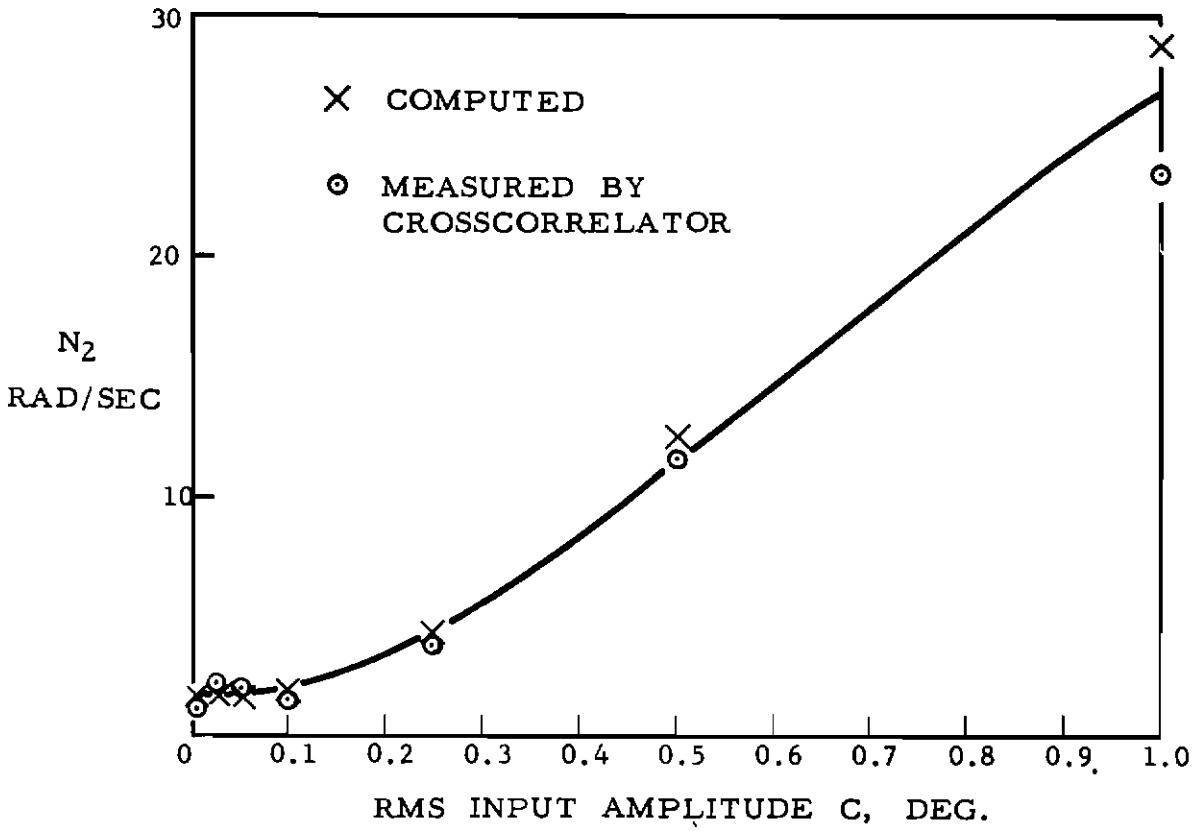

FIGURE 4-9. ACTUATOR TIME CONSTANT VS. INPUT NOISE AMPLITUDE